

การศึกษาเชิงทฤษฎีของการเกิดแสงเช็คกันฮาร์โมนิกตามแนวสะท้อน  
จากผลึกแอมโมเนียมไดไฮโดรเจนฟอสเฟต

นางสาวอุบล สุริพล

วิทยานิพนธ์นี้เป็นส่วนหนึ่งของการศึกษาตามหลักสูตรปริญญาวิทยาศาสตรมหาบัณฑิต

สาขาวิชาเทคโนโลยีเลเซอร์และฟotonิกส์

มหาวิทยาลัยเทคโนโลยีสุรนารี

ปีการศึกษา 2543

ISBN 974-7359-58-8

**THORETICAL STUDY OF REFLECTED SECOND-HARMONIC  
GENERATION IN AMMONIUM DIHYDROGEN  
PHOSPHATE (ADP) CRYSTAL**

Miss Ubon Suripon

A Thesis Submitted in Partial Fulfillment of the Requirements for the  
Degree of Master of Science in Laser Technology and Photonics

Suranaree University of Technology

Academic Year 2000

ISBN 974-7359-58-8

**Thesis Title**

**Theoretical study of reflected second-harmonic generation in  
Ammonium Dihydrogen Phosphate (ADP) crystal**

Suranaree University of Technology Council has approved this thesis submitted in partial fulfillment of the requirements for a Master's Degree.

Thesis Examining Committee

.....  
(Prof. Dr. Vutthi Bhanthumnavin)  
Chairman

.....  
(Prof. Dr. Vutthi Bhanthumnavin)  
Thesis Advisor

.....  
(Asst. Prof. Dr. Joewono Widjaja)  
Member

.....  
(Asst. Prof. Dr. Arjuna Chaiyasena)  
Member

.....  
(Assoc. Prof. Dr. Kasem Prabripataloong)  
Vice Rector for Academic Affairs

.....  
(Assoc. Prof. Dr. Tassanee Sukosol)  
Dean/Institute of Science

นางสาวอุบล สุริพล: การศึกษาเชิงทฤษฎีของการเกิดแสงเช็คกันฮาร์โมนิกตามแนวสะท้อนจากผลึกแอมโมเนียมไดไฮโดรเจนฟอสเฟต (THEORETICAL STUDY OF REFLECTED SECOND-HARMONIC GENERATION IN AMMONIUM DIHYDROGEN PHOSPHATE (ADP) CRYSTAL) อ. ที่ปรึกษา: ศ. ดร. วุฑฒิ พันธุมนาวิน, 75 หน้า.  
ISBN 974-7359-58-8

วิทยานิพนธ์นี้เป็นการศึกษาเชิงทฤษฎีของการเกิดแสงเช็คกันฮาร์โมนิกตามแนวสะท้อนจากผลึก ADP ซึ่งวางตัวอยู่ในของเหลว วัน-โบรโมเนฟธาไลน์ ที่มีค่าดัชนีหักเหมากกว่าผลึก โดยอาศัยแสงเลเซอร์แบบช่วงสั้นมากที่มีความยาวคลื่น 900 นาโนเมตรเป็นตัวกระตุ้นให้เกิด ความเข้มของแสงเช็คกันฮาร์โมนิกจะถูกคำนวณโดยโปรแกรมคอมพิวเตอร์  $C^{++}$  ทั้งนี้ใช้ทฤษฎีของ Bloembergen และ Pershan (1962) เป็นพื้นฐาน ได้มีการพบว่าความเข้มของแสงเช็คกันฮาร์โมนิกในแนวสะท้อนมีค่ามากที่สุดที่มุมตกกระทบวิกฤตภายใต้สภาวะเฟสแมชชิง (phase-matching) และในทางตรงกันข้าม มีการพบว่าเกิดการเกิดแสงเช็คกันฮาร์โมนิกในแนวสะท้อนมีค่าน้อยที่สุดที่สภาวะมุมนอนลิเนียร์บริวสเตอร์ (Nonlinear Brewster angle) โดยในการศึกษาการเกิดมุมนอนลิเนียร์บริวสเตอร์ได้กำหนดลักษณะการวางตัวของผลึกโดยให้แกนออปติคของผลึกทำมุมกับผิวตกกระทบของผลึกในแบบต่างๆ เช่น  $42.68^\circ$ ,  $30^\circ$ ,  $90^\circ$  และ  $0^\circ$  ซึ่งพบว่ามุมนอนลิเนียร์บริวสเตอร์ มีค่าเท่ากับ  $42.02^\circ$ ,  $52.60^\circ$ ,  $0^\circ$  และ  $69.93^\circ$  ตามลำดับ จากผลทางทฤษฎีแสดงให้เห็นว่ามุมนอนลิเนียร์บริวสเตอร์สามารถเกิดได้หลายค่าในผลึกเดียวกัน ทั้งนี้ขึ้นกับลักษณะการวางตัวของผลึก

|                             |                                     |
|-----------------------------|-------------------------------------|
| สาขาวิชาเทคโนโลยีเลเซอร์และ | ลายมือชื่อนักศึกษา.....             |
| โฟตอนิกส์                   | ลายมือชื่ออาจารย์ที่ปรึกษา.....     |
| ปีการศึกษา 2543             | ลายมือชื่ออาจารย์ที่ปรึกษาร่วม..... |
|                             | ลายมือชื่ออาจารย์ที่ปรึกษาร่วม..... |



## Acknowledgments

I would like to express my deep appreciation to the following persons:

Professor Dr. Vutthi Bhanthumnavin, my thesis advisor for his helpful suggestions, support, and encouragement throughout my studies. His generosity is most appreciated.

Asst. Prof. Dr. Arjuna Chaiyasena and Asst. Prof. Dr. Joewono Widjaja, the thesis co-advisors, who patiently read the manuscript and kindly offered suggestions for improvement. Thanks for their kind endurance.

Mr. Chongrit Kumyod, my colleague, who was very kind and helpful in everything I asked for help.

Mr. Satidchok Phosa-ard, whose talent and skillfulness in computer programming tremendously helped me, so that the computer C<sup>++</sup> programs for this research were realizable.

All the friends of mine at the National Synchrotron Research Center for teaching me AutoCAD and everyone else who supported me with available computers.

I am especially grateful to my mother and all the rest of my relatives for their love and trust in me.

Miss Ubon Suripon

# Contents

|  | Page |
|--|------|
| <b>Abstract (Thai)</b> .....   | I    |
| <b>Abstract (English)</b> .....  | II   |
| <b>Acknowledgements</b> .....  | III  |
| <b>Contents</b> .....  | IV   |
| <b>List of Tables</b> .....  | VII  |
| <b>List of Figures</b> .....   | VIII |
| <b>List of Symbols</b> .....   | IX   |
| <b>Chapter I Introduction</b> .....  | 1    |
| 1.1 Introduction: Literature Review.....                                       | 1    |
| 1.2 Objective .....  | 3    |
| 1.3 Hypothesis.....  | 4    |
| 1.4 Organization of the Thesis.....  | 4    |
| <b>Chapter II Theory of Second-harmonic Generation</b> .....                   | 6    |
| 2.1 Introduction.....  | 6    |
| 2.2 Second-harmonic Generation.....  | 6    |
| 2.2.1 Wave equation in nonlinear medium.....                                   | 9    |
| 2.2.2 Generalized Snell's law.....   | 13   |
| 2.2.3 Polarization and intensity of the reflected<br>second-harmonic wave..... | 16   |
| 2.2.4 Second-harmonic generation at total reflection.....                      | 18   |

## Contents (Continued)

|  | Page      |
|--|-----------|
| 2.2.5 Phase-matching in second-harmonic generation.....  | 23        |
| 2.2.6 Nonlinear Brewster angle.....  | 25        |
| <b>Chapter III Procedure</b> .....   | <b>27</b> |
| 3.1 Introduction.....  | 27        |
| 3.2 Ultrashort pulse laser.....  | 28        |
| 3.3 ADP Crystal.....   | 29        |
| 3.4 Liquid 1-bromonaphthalene.....   | 30        |
| 3.5 Computation of Relative Reflected second-harmonic Intensity .....  | 30        |
| 3.5.1 The calculation of refractive indices of extraordinary<br>ray, $n_e^{2\omega}(\theta)$ .....                                     | 32        |
| 3.5.2 The calculation of relative reflected second-harmonic<br>intensity (SHI).....  | 33        |
| <b>Chapter IV Result and Discussion</b> .....  | <b>36</b> |
| 4.1 Introduction.....  | 36        |
| 4.2 Phase-matched Second-harmonic Generation.....  | 36        |
| 4.3 Nonlinear Brewster Angle.....  | 37        |
| 4.3.1 Nonlinear Brewster angle of ADP with $P^{NLS}(2\omega)$<br>making an angle $\theta_m = 42.68^\circ$ with the incident surface... | 39        |
| 4.3.2 Nonlinear Brewster angle of ADP with $P^{NLS}(2\omega)$<br>making an angle $30^\circ$ with the incident surface.....             | 41        |

## Contents (Continued)

|   | Page |
|---|------|
| 4.3.3 Nonlinear Brewster angle of ADP with $P^{NLS}(2\omega)$                           |      |
| lies along the face normal.....   | 43   |
| 4.3.4 Nonlinear Brewster angle of ADP at total reflection.....                          | 45   |
| <b>Chapter V Conclusion</b> .....   | 48   |
| <b>References</b> .....   | 51   |
| <b>Appendixes</b> .....   | 55   |
| Appendixes A Derivation of Refractive indices of 1-bromonaphthalene...                  | 56   |
| Appendix B C <sup>++</sup> Program for Calculate Relative Reflected SHI.....            | 59   |
| B.1 $P^{NLS}(2\omega)$ making at $\theta_m = 42.68^\circ$ with the incident surface.... | 59   |
| B.2 $P^{NLS}(2\omega)$ making at $30^\circ$ with the incident surface.....              | 63   |
| B.3 $P^{NLS}(2\omega)$ making at $0^\circ$ with the face normal.....                    | 67   |
| B.4 $P^{NLS}(2\omega)$ making at $90^\circ$ with the face normal.....                   | 71   |
| <b>Biography</b> .....  | 75   |

## List of Tables

| <b>Table</b>  | <b>Page</b> |
|---|-------------|
| 5.1 The summarized results of reflected SHI of ADP<br>with different aspect of crystallographic cuts..... | 49          |
| A.1 The sets of wavelength and indices $n$ , used for<br>the calculation of $n_{iq}(\omega)$ .....        | 58          |
| A.2 The sets of wavelength and indices $n$ , used for<br>the calculation of $n_{iq}(2\omega)$ .....       | 58          |

## List of Figures

| Figure   | page |
|--|------|
| 2.1 The geometric situation of linear optical interaction.....   | 7    |
| 2.2 The geometric situation of second-harmonic generation<br>based on the nonlinear optical interaction.....   | 8    |
| 2.3 The incident, reflected, and transmitted wave at the fundamental<br>and second-harmonic frequencies at the boundary between vacuum<br>and ADP crystal.....   | 12   |
| 2.4 Schematic representation of two incident waves at frequencies $\omega_1$<br>and $\omega_2$ traveling from a linear medium induces a reflected wave,<br>a homogeneous and inhomogeneous transmitted wave at the<br>sum frequency $\omega_3 = \omega_1 + \omega_2$ ..... | 14   |
| 2.5 The second-harmonic wave with the electric field vector<br>parallel to the plane of incidence.....   | 17   |
| 2.6 The incident, reflected and transmitted rays at fundamental and<br>second-harmonic frequencies in the vicinity of critical angle.....  | 20   |
| 2.7 The refractive index for ordinary and extraordinary rays in a negative<br>uniaxial crystal. The condition of phase-matching is satisfied at $\theta_m$ ...   | 24   |
| 2.8 The physical interpretation of nonlinear Brewster angle.....   | 26   |
| 3.1 Geometry illustrates the crystallographic axes system $(x, y, z)$ .....  | 27   |
| 3.2 Flowchart for theoretical calculation of SHI in reflection.....  | 31   |

## List of Figures (Continued)

| Figure   | page |
|--|------|
| 3.3 The variation of $n_e^{2\omega}(\theta)$ as a function of $\theta$ .....   | 32   |
| 3.4 Process for computing of SHI in reflection.....  | 34   |
| 4.1 Relative reflected second-harmonic intensity (SHI) from ADP crystal<br>as a function of $\theta_i$ with phase-matching at total reflection<br>$\theta_{cr}(\omega) = \theta_{cr}(2\omega) = 67.76^\circ$ .....                                     | 38   |
| 4.2 Relative reflected second-harmonic intensity (SHI) from ADP crystal<br>as a function $\theta_i$ . Nonlinear Brewster angle is at $\theta_i^{NB} = 42.02^\circ$ with<br>$P^{NLS}(2\omega)$ is at $42.68^\circ$ from the incident surface.....       | 40   |
| 4.3 Relative reflected second-harmonic intensity (SHI) from ADP crystal<br>as a function $\theta_i$ . Nonlinear Brewster angle is at $\theta_i^{NB} = 52.6^\circ$ with<br>$P^{NLS}(2\omega)$ is at $30^\circ$ from the incident surface.....           | 42   |
| 4.4 Relative reflected second-harmonic intensity (SHI) from ADP crystal<br>as a function $\theta_i$ . Nonlinear Brewster angle is at $\theta_i^{NB} = 0^\circ$ with<br>$P^{NLS}(2\omega)$ lies along the face normal.....                              | 44   |
| 4.5 Relative reflected second-harmonic intensity (SHI) from ADP crystal<br>as a function $\theta_i$ . Nonlinear Brewster angle is at $\theta_i^{NB} = \theta_{cr}(2\omega) = 70^\circ$<br>with $P^{NLS}(2\omega)$ lies along the incident surface..... | 46   |

## List of Symbols

|                                     |  |
|-------------------------------------|--|
| $A_R$                               | = cross-section area   |
| $dd'$                               | = area of the rectangular slit                                 |
| $\vec{E}$                           | = electric field   |
| $\vec{E}(\omega)$                   | = electric field of fundamental wave $\omega$                  |
| $E_o$                               | = electrical amplitude of fundamental wave                     |
| $\vec{E}_2 \equiv \vec{E}(2\omega)$ | = electric field of second-harmonic wave                       |
| $E^i(\omega)$                       | = electric field of incident fundamental wave                  |
| $E^t(\omega)$                       | = electric field of transmitted fundamental wave               |
| $E_1^t$                             | = electrical amplitude of transmitted fundamental wave         |
| $E^r(\omega)$                       | = electric field of reflected fundamental wave                 |
| $\vec{E}_2^T \equiv E^T(2\omega)$   | = electric field of transmitted second-harmonic wave           |
| $\vec{E}_2^R \equiv E^R(2\omega)$   | = electric field of reflected second-harmonic wave             |
| $E_2^T$                             | = electrical amplitude of transmitted second-harmonic wave     |
| $E_2^R$                             | = electrical amplitude of reflected second-harmonic wave       |
| $E_{//}^T$                          | = electrical amplitude of transmitted second-harmonic wave     |
| $E_{//}^R$                          | = electrical amplitude of reflected second-harmonic wave       |
| $\hat{e}_T$                         | = polarization unit vector of transmitted second-harmonic wave |
| $\hat{e}_R$                         | = polarization unit vector of reflected second-harmonic wave   |
| $F_T^L$                             | = Linear Fresnel factor  |

## List of Symbols (Continued)

|                        |  |
|------------------------|--|
| $F_{R,\parallel}^{NL}$ | = nonlinear Fresnel factor   |
| $\vec{H}$              | = magnetic field   |
| $\vec{H}_2^T$          | = magnetic field of transmitted second-harmonic wave               |
| $\vec{H}_2^R$          | = magnetic field of reflected second-harmonic wave                 |
| $I_R(2\omega)$         | = reflected second-harmonic intensity                              |
| $\vec{k}$              | = wave vector  |
| $\vec{k}_1^i$          | = wave vector incident wave at $\omega_1$                          |
| $\vec{k}_2^i$          | = wave vector incident wave at $\omega_2$                          |
| $\vec{k}_2^R$          | = wave vector reflected second-harmonic wave                       |
| $\vec{k}^S$            | = wave vector of source term                                       |
| $\vec{k}_2^T$          | = wave vector of homogeneous transmitted wave                      |
| $\vec{k}_1^t$          | = wave vector transmitted wave at $\omega_1$                       |
| $\vec{k}_2^t$          | = wave vector transmitted wave at $\omega_2$                       |
| $k_3^R$                | = wave vector reflected wave at $\omega_3 = \omega_1 + \omega_2$   |
| $k_3^S$                | = wave vector source term at $\omega_3 = \omega_1 + \omega_2$      |
| $k_3^T$                | = wave vector transmitted wave at $\omega_3 = \omega_1 + \omega_2$ |
| $n$                    | = index of refraction  |
| $n_{liq}$              | = refractive index of 1-bromonaphthalene                           |
| $n_o$                  | = refractive index of ordinary ray                                 |
| $n_e$                  | = refractive index of extraordinary ray                            |

## List of Symbols (Continued)

|                          |  |
|--------------------------|--|
| $n_e^{2\omega}(\theta)$  | = refractive index of extraordinary ray at any angle $\theta$    |
| $\bar{P}$                | = polarization   |
| $\hat{p}$                | = polarization unit vector                                       |
| $\bar{P}^{NLS}(2\omega)$ | = nonlinear polarization   |
| $P_{//}^{NLS}$           | = magnitude of nonlinear polarization in the plane of reflection |
| $\alpha$                 | = angle between $\bar{P}^{NLS}(2\omega)$ and $\bar{k}^S$         |
| $\lambda$                | = wavelength   |
| $\chi^{(1)}$             | = linear susceptibility  |
| $\chi^{(2)}$             | = second-order nonlinear susceptibility                          |
| $\omega$                 | = frequency  |
| $\epsilon$               | = dielectric constant  |
| $\theta$                 | = angle between propagation vector and optic axis                |
| $\theta_i$               | = incident angle   |
| $\theta_i^{NB}$          | = nonlinear Brewster angle                                       |
| $\theta_r$               | = reflected angle of fundamental ray                             |
| $\theta_{cr}(\omega)$    | = critical angle which cause $\bar{k}^S = 90^\circ$              |
| $\theta_{cr}(2\omega)$   | = critical angle which cause $\bar{k}^T = 90^\circ$              |
| $\theta_R$               | = reflected angle of second-harmonic wave                        |
| $\theta_S$               | = transmitted angle of ray with wave vector $\bar{k}^S$          |
| $\theta_T$               | = transmitted angle of ray with wave vector $\bar{k}^T$          |

**List of Symbols (Continued)**

|            |  |
|------------|--|
| $\theta_m$ | = phase-matching angle   |
| $\varphi$  | = angle between two plane of incidence                                       |
| $\gamma$   | = angle between optic axis ( $\bar{P}^{NLS}(2\omega)$ ) and incident surface |

# Chapter I

## Introduction

### 1.1 Introduction:Literature Review

The field of nonlinear optics is the study of the interactions of laser light with matter when the response of material system to an applied electromagnetic field is nonlinear. The beginning of nonlinear optics took place with the first observation of second harmonic light of the ruby laser in quartz crystal (Franken, Hill, Peters, and Weinreich, 1961). It has been rapidly growing since the early 1960s soon after the invention of the laser (Maiman, 1960). The high intensity of laser light was utilized as a coherent light source making available experimental observations of nonlinear optical phenomena which cannot occur in conventional (linear) optics. The most interesting of such phenomena is second harmonic generation in which the light wave of frequency  $\omega$  propagating through a crystal lacking inversion symmetry is converted to light wave at  $2\omega$ . Second harmonic generation in transmission was first discovered by Franken et al. (1961) by focusing the red light ( $\lambda = 694 \text{ nm}$ ) from ruby laser onto the quartz crystal, resulting in the blue light ( $\lambda = 347 \text{ nm}$ ) generated at a second harmonic frequency. However, the conversion efficiency from  $\omega$  to  $2\omega$  was relatively small. The achievement of maximum intensity of transmitted second harmonic generation can be performed by phase-matching technique (Maker, Terhune, Nisenoff, and Savage, 1962; Giordmaine, 1962; Ashkin, Boyd, and Dziedzic, 1963; Boyd, Ashkin, Dziedzic, and Kleinman, 1965; Bhanthumnavin and Lee, 1994).

Bloembergen and Pershan (1962) first theoretically demonstrated the behavior of second harmonic wave such as the refraction and reflection, at the boundary of a nonlinear media. Their work also included the generalized Snell's law, which showed the relation between the incident, reflected and transmitted angles of both fundamental beam and second harmonic beams. The analysis of total reflection and Brewster angle phenomena were given as well. In 1963, Ducuing and Bloembergen (1963) performed an experimental verification of the law for second harmonic light in reflection. Many aspects of the Bloembergen and Pershan (BP) theory have been verified in different experimental situations. The most important aspects of BP theory were concerned with primary beam incidents from an optically denser medium to a lesser dense nonlinear medium. In this case, total reflection of primary beam and second harmonic beam will occur, as demonstrated by Bloembergen, Simon, and Lee (1969) in particular, for non-phase-matched second harmonic at total reflection. The phase-matched second harmonic at total reflection leads to enhancement of the reflected second-harmonic intensity at critical angle (Bloembergen and Lee, 1967; Lee and Bhanthumnavin, 1976; Bhanthumnavin and Lee, 1994). In addition, there is an interesting phenomenon, which occurs when the primary beam is incident upon a nonlinear medium at particular angle of incident called nonlinear Brewster angle. At this angle, the reflected second harmonic intensity vanishes. This phenomenon was first experimentally demonstrated by Chang and Bloembergen (1966) in GaAs crystal for opaque medium in which the vanishing of reflected second harmonic light could not be observed clearly. Later Lee and Bhanthumnavin (1976) first observed the nonlinear Brewster angle in transparent medium KDP crystal. In 1994, Bhanthumnavin and Lee (1994) performed experimental observations of the nonlinear

Brewster angle and the phase matched second harmonic at total reflection of KDP crystal by using a mode-locked neodymium glass laser. However, the nonlinear Brewster angle can occur at other crystallographic orientations of the crystal because the occurrence of nonlinear Brewster angle depends on the inclination of nonlinear polarization  $P^{NLS}(2\mathbf{w})$ , which lies in the plane of incidence. The theoretical prediction of nonlinear Brewster angle in ADP crystal immersed in the optically denser liquid 1-Bromonaphthalene by using the Nd:YAG laser of  $\lambda = 1064$  nm as a fundamental beam was reported by Bhanthumnavin and Ampole (1990) also for KDP crystal reported by Suripon and Bhanthumnavin (1999). Besides the null intensity of second harmonic in reflection, the null intensity in transmission, which does not occur in linear optic, has also been observed (Bhanthumnavin and Lee, 1994; Dürr, Hildebrandt, Marowsky, and Stolle, 1997).

## 1.2 Objective

In order to extend the field of nonlinear optics, especially in the area of second harmonic generation in reflection, this thesis is devoted to the theoretical investigation of reflected second harmonic intensity generated from ADP crystal. The ultrashort pulse laser at wavelength  $\lambda = 900$  nm with high peak power output will be utilized as the fundamental beam. The maximum and minimum intensity of reflected second harmonic lights are obtained through phase matching technique, and for the condition of nonlinear Brewster angle, respectively. Such intensity is calculated by computer simulation (using C++ program) based on the theory of Bloembergen and Pershan (1962). Different crystallographic orientations of the ADP crystal will be used to

determine the intensity of reflected second harmonic generation under ultrashort laser pulse excitation. The nonlinear Brewster angle dependence on the crystallographic orientation will be investigated. Unlike the previous studies, in which the crystallographic orientation of the crystals either had their optic axis ( $P^{NLS}(2\mathbf{w})$ ) inclining with respect to their incident surface at  $82^\circ$  (GaAs crystal by Chang and Bloembergen, 1966);  $42.05^\circ$  (ADP crystal by Bhanthumnavin and Ampole, 1990);  $41.2^\circ$  (KDP crystal by Bhanthumnavin and Lee, 1994); or  $30^\circ$  (KDP crystal by Suripon and Bhanthumnavin, 1999), the crystallographic cuts used in the thesis are  $42.68^\circ$ ,  $30^\circ$ ,  $0^\circ$  and  $90^\circ$ .

### 1.3 Hypothesis

Under the newly proposed crystal orientation cuts, it is expected to achieve the condition of nonlinear Brewster angle and phase matching condition at total reflection by using ultrashort pulse laser at  $\lambda = 900$  nm. Unlike the linear case, the nonlinear Brewster angle dependence on crystallographic orientations is not unique. The test of hypothesis can be done by comparing our result with the previous studies in which the nonlinear medium has same crystal class as KDP and ADP crystals.

### 1.4 Organization of the Thesis

This paper is organized as follows.

Chapter 1: Introduction. This chapter presents the background and reviews the history of second-harmonic generation. The research objective and hypothesis are also given.

Chapter 2: Theory of Second-harmonic generation. This chapter will focus on second-harmonic generation in reflection. The concept of both phase-matching at total reflection and nonlinear Brewster angle are discussed.

Chapter 3: Procedure. The chapter is for the theoretical preparation of ADP crystal cut and selection of optically denser fluid in order to enable for total reflection. The computer C++ program used for the theoretical calculation of relative reflected second-harmonic intensity will be discussed as well.

Chapter 4: Results and Discussion. In this chapter, results of second-harmonic harmonic generation via phase-matched technique as well as ADP crystallographic cuts in order to obtain nonlinear Brewster angles are well described, analyzed and plotted in semi-logarithmic scale.

Chapters 5 conclusions of the results as well as suggestion for future research are presented.

## **Chapter II**

### **Theory of Second-harmonic Generation**

#### **2.1 Introduction**

In this chapter, the theory of optical second-harmonic generation will be presented. The propagation of second-harmonic waves governed by Maxwell's equations with the incorporation of nonlinear polarization is described by the Bloembergen and Pershan (1962) theory. The general law of refraction and reflection which gives the direction of the harmonic waves that emanate from the boundary of nonlinear medium are derived. The intensity of second-harmonic in reflection described by the nonlinear Fresnel factor that actually depends on the incident angle of the fundamental beam is demonstrated. The achievement of both maximum and minimum of reflected second harmonic intensity via phase-matching and nonlinear Brewster angle, respectively, are also theoretically carried out.

#### **2.2 Second-harmonic Generation**

One type of the interaction of light wave with matter is the effect of electric field on the polarization ( $\vec{P}$ ) or dipole moment per unit volume within a material. In case of linear optics, the induced polarization depends linearly on the applied electric field, which can be described by the relationship

$$\vec{P} = \epsilon^{(1)} \vec{E}, \quad (2.1)$$

where the constant of proportionality  $\epsilon^{(1)}$  is known as the linear susceptibility. This induced polarization acts as the source of new electromagnetic wave radiating in both transmitted and reflected direction, with same characteristic as the applied field as shown in Figure 2.1. Linear optical phenomena, such as the refraction, reflection, dispersion, as well as birefringence of light propagation in a medium are based on this relation.

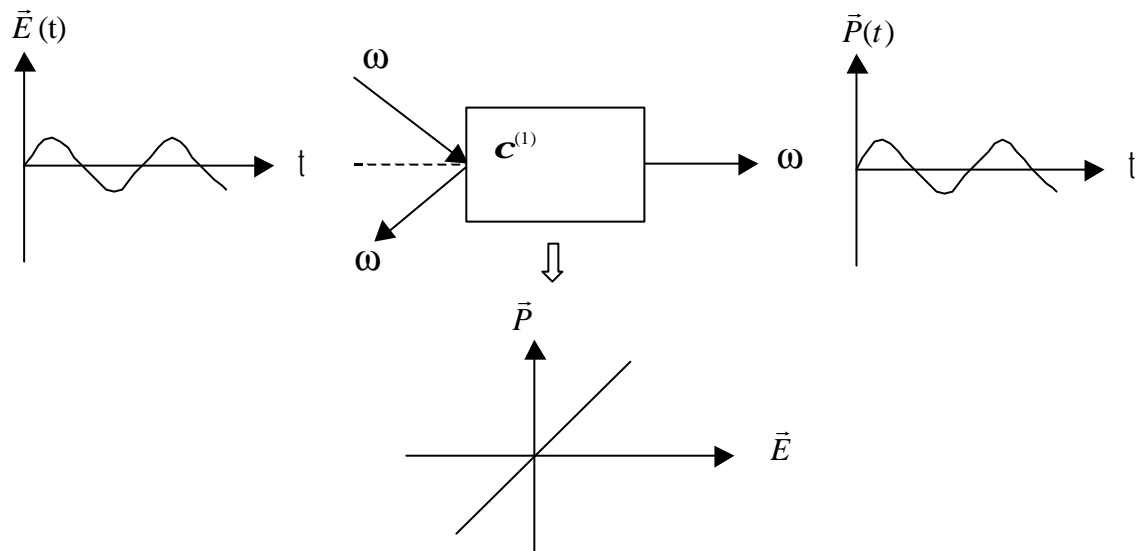


Figure 2.1. The geometric situation of linear optical interaction.

However, Linear optical interaction is only applicable for low applied electric field strengths. The existence of nonlinear optical phenomena in materials should occur when a high electric field is applied. The nonlinear optics concepts can be found in several textbooks (Bloembergen, 1965; Butcher and Cotter, 1990; Prasad and Williams, 1990; Mills, 1991; Boyd, 1992; Newell and Moloney, 1992; He and Liu, 1999). The induced nonlinear polarization within material can be expressed as the power series of the applied electric field

$$\vec{P} = \mathbf{c}^{(1)}\vec{E} + \mathbf{c}^{(2)}:\vec{E}\vec{E} + \dots, \quad (2.2)$$

where  $\mathbf{c}^{(2)}$  known as the second order susceptibility, a tensor quantity the whose components provide the response for a given orientation of the crystallographic axes relative to the incident field. The second order nonlinear polarization results in optical nonlinear phenomena, such as second-harmonic generation (SHG), sum - frequency generation (SFG) and difference frequency generation (DFG). Here, we will concentrate in detail only on second-harmonic generation, where a coherent optical wave of frequency  $\omega$  can induce a new coherent wave radiation at frequency  $2\omega$  in noncentrosymmetric crystal. Figure 2.2 shows the process of second-harmonic generation. The induced nonlinear polarization consists of the second-harmonic of  $\omega$ , fundamental frequency ( $\omega$ ) and an average (dc) term.

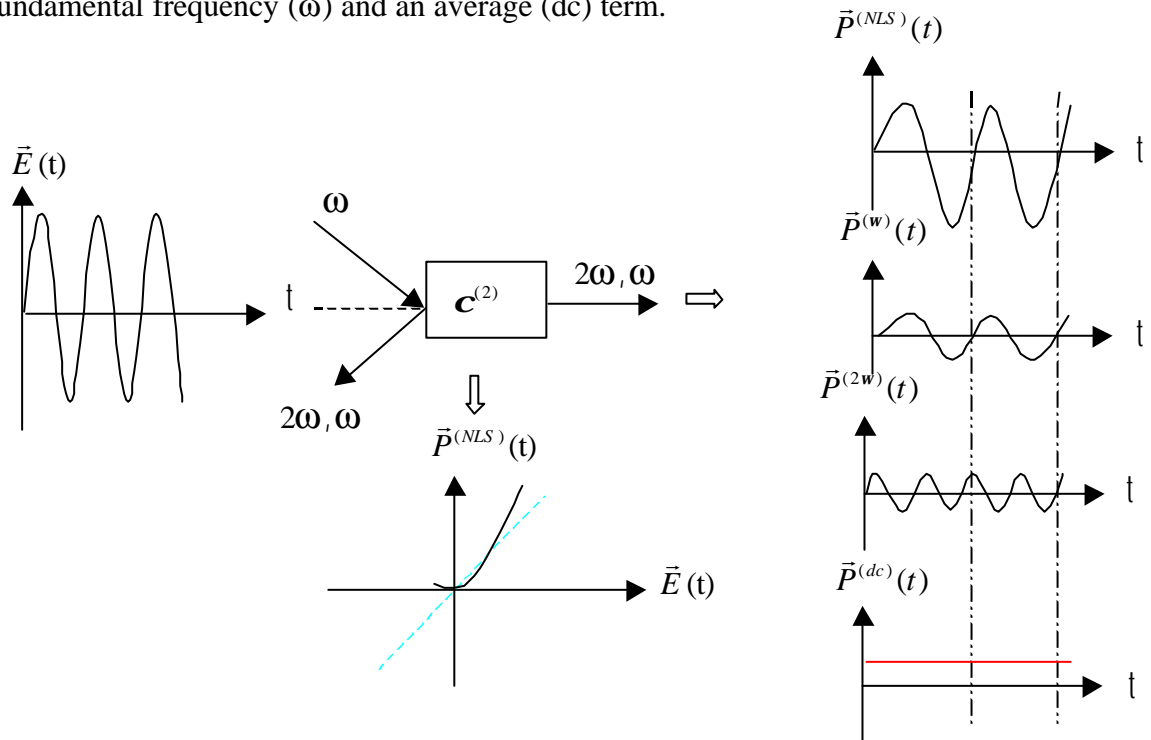


Figure 2.2. The geometric situation of second-harmonic generation based on the nonlinear optical interaction.

For second harmonic generation, the nonlinear polarization can be rewritten in vector notation by

$$\bar{P}^{NLS}(\mathbf{2}\boldsymbol{\omega}) = \mathbf{c}^{(2)} : \bar{E}(\boldsymbol{\omega})\bar{E}(\boldsymbol{\omega}), \quad (2.3)$$

or in the matrix form of a third order tensor (that  $\mathbf{c}_{ijk}^{(2)}$  has  $3 \times 6 = 18$  elements)

$$\begin{bmatrix} P_x^{NLS}(\mathbf{2}\boldsymbol{\omega}) \\ P_y^{NLS}(\mathbf{2}\boldsymbol{\omega}) \\ P_z^{NLS}(\mathbf{2}\boldsymbol{\omega}) \end{bmatrix} = \begin{bmatrix} \mathbf{c}_{xxx}^{(2)} & \mathbf{c}_{xyy}^{(2)} & \dots & \mathbf{c}_{xxy}^{(2)} \\ \mathbf{c}_{yxx}^{(2)} & \mathbf{c}_{yyy}^{(2)} & \dots & \mathbf{c}_{yyx}^{(2)} \\ \mathbf{c}_{zxx}^{(2)} & \mathbf{c}_{zyy}^{(2)} & \dots & \mathbf{c}_{zxy}^{(2)} \end{bmatrix} \begin{bmatrix} E_x^2(\boldsymbol{\omega}) \\ E_y^2(\boldsymbol{\omega}) \\ E_z^2(\boldsymbol{\omega}) \\ 2E_y(\boldsymbol{\omega})E_z(\boldsymbol{\omega}) \\ 2E_x(\boldsymbol{\omega})E_z(\boldsymbol{\omega}) \\ 2E_x(\boldsymbol{\omega})E_y(\boldsymbol{\omega}) \end{bmatrix}, \quad (2.4)$$

or, equivalently,

$$\bar{P}_i^{NLS}(\mathbf{2}\boldsymbol{\omega}) = \sum_{j,k} \mathbf{c}_{ijk}^{(2)} \bar{E}_j(\boldsymbol{\omega})\bar{E}_k(\boldsymbol{\omega}), \quad (2.5)$$

where  $x, y, z$  are of a cartesian coordinate system;  $P_x^{NLS}(\mathbf{2}\boldsymbol{\omega}), E_x(\boldsymbol{\omega})$ , etc., are the components of the vectors  $\bar{P}^{NLS}(\mathbf{2}\boldsymbol{\omega})$  and  $\bar{E}(\boldsymbol{\omega})$ , respectively. Here  $\omega$  is actually a parameter rather than an argument showing a true functional dependence. It is clear that  $P_z^{NLS}(\mathbf{2}\boldsymbol{\omega})$  will be induced along  $z$ -axis inside the medium if the fundamental field is polarized along the  $xy$ -plane ( $E_z(\boldsymbol{\omega}) = 0$ ). It is important to note that the second-harmonic can be generated from only noncentrosymmetric crystal in which its crystal structure lacking inversion symmetry, such as GaAs, CdTe, KDP, ADP crystals.

### 2.2.1 Wave equations in nonlinear medium

The behavior of the reflection and transmission waves, at the boundary of nonlinear medium has been treated theoretically (Armstrong, Bloembergen, Ducuing,

and Pershan, 1962; Bloembergen and Preshan, 1962). In this section, the derivation of the wave equations of the monochromatic electric field of frequency  $\omega_1$  in a nonlinear medium will be discussed. Restricts us to a transverse plane wave, in the lossless, nonlinear dielectric material. Maxwell equations for the medium with the incorporation of the nonlinear source term  $P^{NLS}$  (Armstrong et al., 1962; Bloembergen and Pershan, 1962), were given as

$$\nabla \times \vec{E} = -\frac{1}{c} \frac{\partial \vec{m}\vec{H}}{\partial t}, \quad (2.6)$$

$$\nabla \times \vec{H} = \frac{1}{c} \frac{\partial (\mathbf{e}\vec{E})}{\partial t} + \frac{4\mathbf{p}}{c} \frac{\partial \vec{P}^{NLS}}{\partial t}, \quad (2.7)$$

where  $\vec{E}$  is the electric field, with components  $(E_x, E_y, E_z)$ , and  $\vec{H}$  is the magnetic field, with components  $(H_x, H_y, H_z)$ ;  $\mathbf{m}$  and  $\mathbf{e}$  are the permeability and permittivity, respectively, of the medium in which the wave is propagating; and  $c$  is the velocity of propagation in vacuum.  $\vec{E}$ ,  $\vec{H}$ , and  $\vec{P}^{NLS}$  are functions of both position  $(x, y, z)$  and time  $t$ .

If the medium is nonmagnetic and homogeneous (constant  $\epsilon$ ),  $\mathbf{m}=1$  and  $\mathbf{e}$  will be taken as a scalar quantity. Combining the Maxwell's equations. (2.6) and (2.7) leads to a wave equation contained with a nonlinear polarization source

$$\nabla \times \nabla \times \vec{E} + \frac{\mathbf{e}}{c^2} \frac{\partial^2 \vec{E}}{\partial t^2} = -\frac{4\mathbf{p}}{c^2} \frac{\partial^2 \vec{P}^{NLS}}{\partial t^2}. \quad (2.8)$$

The wave at second-harmonic frequency  $\omega_2 = 2\omega_1$  generated by  $\vec{P}^{NLS}$  within the medium will obey this equation. Choose the coordinate system in such a way that the boundary is given by  $z = 0$ , the plane of incidence (that plane which contains both the incident, refracted and reflected wave vectors) given by  $xz$ -plane. The wave

vectors  $k_1^i$  and  $k_1^r$  are incident and refracted ray, respectively. The time-space function of the induced nonlinear source term at second-harmonic frequency is given by

$$\begin{aligned}\bar{P}^{NLS} &= \hat{p}P^{NLS}(2\mathbf{w}_1) \\ &= \mathbf{C}(2\mathbf{w}_1) : \bar{E}_1^i \bar{E}_1^r \exp i(\bar{k}^s \cdot \bar{r} - 2\mathbf{w}_1 t),\end{aligned}\quad (2.9)$$

where  $E_1^r$  is the amplitude of the refracted ray at the fundamental frequency and  $\hat{p}$  is a nonlinear polarization unit vector. The wave vector of the nonlinear source term is twice the wave vector of the refracted fundamental ray,  $\bar{k}^s = 2\bar{k}_1^r$ . It is meaningful to write the Maxwell's equation for second-harmonic wave as

$$\nabla^2 \bar{E}_2 - \frac{\mathbf{e}(2\mathbf{w}_1)}{c^2} \frac{\partial^2 \bar{E}_2}{\partial t^2} = \frac{4\mathbf{p}}{c^2} \frac{\partial^2 \bar{P}^{NLS}(2\mathbf{w}_1)}{\partial t^2}.$$
 (2.10)

This is an inhomogeneous differential equation, whose general solution consists of the homogeneous equation plus one particular solution of the inhomogeneous equation,

$$\begin{aligned}\bar{E}_2^T &= \hat{e}_T E_2^T \exp i(\bar{k}_2^T \cdot \bar{r} - 2\mathbf{w}_1 t) - \frac{4\mathbf{p}^{NLS}(4\mathbf{w}_1^2/c^2)}{(k_2^T)^2 - (k^s)^2} \\ &\times \left[ \hat{p} - \frac{\bar{k}^s (\bar{k}^s \cdot \hat{p})}{(k_2^T)^2} \right] \exp i(\bar{k}^s \cdot \bar{r} - 2\mathbf{w}_1 t),\end{aligned}\quad (2.11)$$

$$\begin{aligned}\bar{H}_2^T &= \frac{c}{2\mathbf{w}_1} (\bar{k}_2^T \times \hat{e}_T) E_2^T \exp i(\bar{k}_2^T \cdot \bar{r} - 2\mathbf{w}_1 t) \\ &- \frac{4\mathbf{p}^{NLS}(4\mathbf{w}_1^2/c^2)}{(k_2^T)^2 - (k^s)^2} \frac{c}{2\mathbf{w}_1} (\bar{k}^s \times \hat{p}) \exp i(\bar{k}^s \cdot \bar{r} - 2\mathbf{w}_1 t).\end{aligned}\quad (2.12)$$

These expressions represent the time-space function of the second-harmonic field inside the nonlinear medium. The reflected second-harmonic wave can be obtained from the homogeneous differential equation, normally it is the plane wave that propagates in free space,

$$\bar{E}_2^R = \hat{e}_T E_2^R \exp i(\bar{k}_2^R \cdot \bar{r} - 2\mathbf{w}_1 t), \quad (2.13)$$

$$\vec{H}_2^R = \frac{c}{2\mathbf{w}_1} (\vec{k}_2^R \times \hat{e}_T) E_2^R \exp i(\vec{k}_2^R \cdot \vec{r} - 2\mathbf{w}_1 t). \quad (2.14)$$

Applying the boundary conditions, one can resolve the magnitude of the transmitted  $E_2^T$  and reflected  $E_2^R$  amplitudes and the direction of wave vectors of the homogeneous transmitted wave  $\vec{k}_2^T$  and the reflected wave  $\vec{k}_2^R$ , as well as the polarization unit vectors  $\hat{e}_T$  and  $\hat{e}_R$ . It is evident that the nonlinear source term emits the second-harmonic wave in both reflected and transmitted directions, particularly in the anisotropic case there are two transmitted beams, while the linear polarization radiates the fundamental reflected and transmitted beams. Figure 2.3 shows the geometry of wave at the interface of vacuum and ADP crystal.

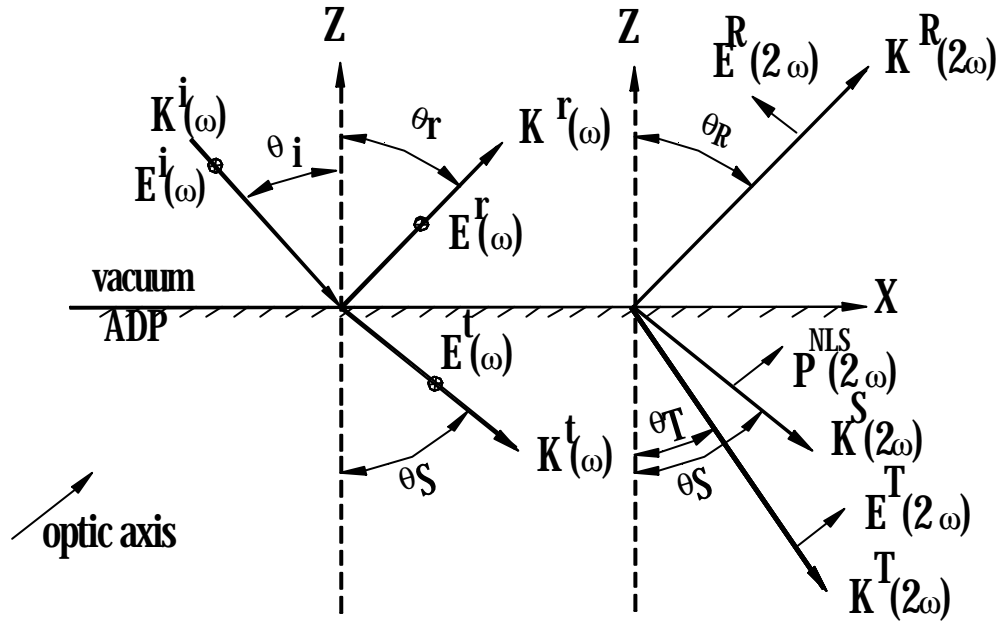


Figure 2.3. The incident, reflected and refracted wave vectors at the fundamental and second-harmonic frequencies at the boundary between vacuum and ADP crystal.

There is no dispersion in vacuum, so that the reflected second-harmonic wave goes in the same direction as the reflected fundamental wave. Since  $\vec{k}^s = 2\vec{k}_1^t$ , the refracted fundamental wave and the inhomogeneous source wave go in the same direction, whereas the homogeneous transmitted second-harmonic wave goes in different direction.

### 2.2.2 Generalized Snell's law

As shown in Figure 2.3, the incident, refracted, and reflected angles of the fundamental and second-harmonic frequencies lie in the plane of incidence. They are related by the generalized Snell's law. The generalized Snell's law was theoretically demonstrated by Bloembergen and Pershan (1962) and was verified experimentally by Ducuing and Bloembergen (1963). The derivation of generalized Snell's law based on Bloembergen and Pershan theory will be discussed in the following.

Consider the boundary between a linear and nonlinear medium with two plane waves,  $\vec{E}_1 \exp i(\vec{k}_1^i \cdot \vec{r} - \mathbf{w}_1 t)$  and  $\vec{E}_2 \exp i(\vec{k}_2^i \cdot \vec{r} - \mathbf{w}_2 t)$  incident from the nonlinear medium as illustrated in Figure 2.4. Letter “I” and “R” indicates the incident and reflected wave at the side of linear medium, respectively, and “T” and “t” indicates the transmitted wave at sum frequency  $\mathbf{w}_3 = \mathbf{w}_1 + \mathbf{w}_2$  and transmitted wave at frequencies  $\mathbf{w}_1$  and  $\mathbf{w}_2$  inside nonlinear medium, respectively. The incident angle of two planes wave are  $\mathbf{q}_1^i$  and  $\mathbf{q}_2^i$ : their plane of incident make an angle  $\mathbf{j}$  with each other.

The proper choice of coordinate system is  $x$  and  $y$  direction such that

$$k_{1y}^i = -k_{2y}^i.$$

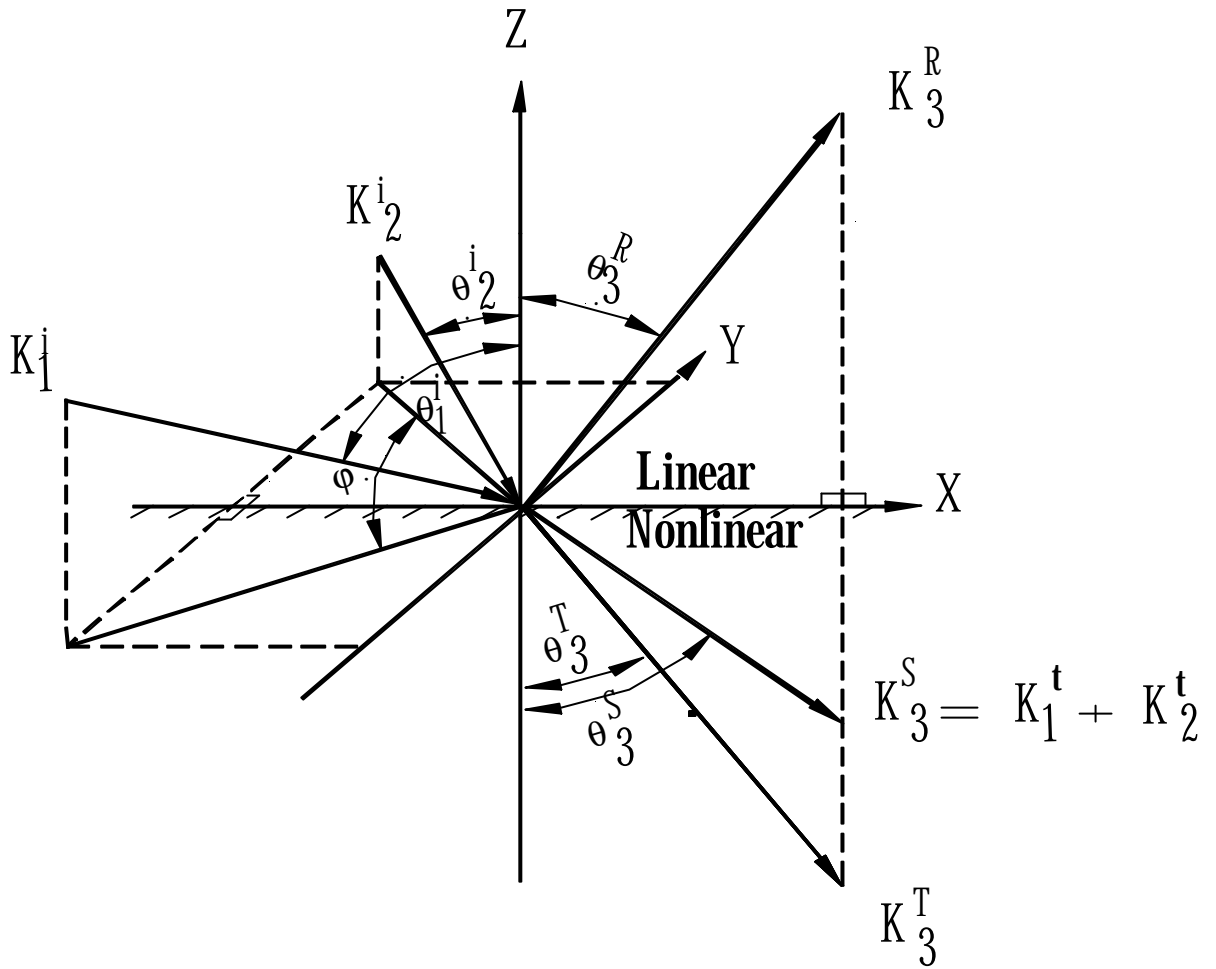


Figure 2.4. Schematic representation of two incident waves at frequencies  $\omega_1$  and  $\omega_2$  traveling from a linear medium induces a reflected wave, a homogeneous and inhomogeneous transmitted wave at the sum frequency  $\omega_3 = \omega_1 + \omega_2$ .

At planar interface ( $z = 0$ ), there is the conservation of the tangential momentum components,

$$k_{3x}^R = k_{3x}^T = k_{3x}^S = k_{1x}^i + k_{2x}^i = k_{1x}^i + k_{2x}^i, \quad (2.15)$$

$$k_{3y}^R = k_{3y}^T = k_{3y}^S = k_{1y}^i + k_{2y}^i = k_{1y}^i + k_{2y}^i = 0. \quad (2.16)$$

These relations show that the inhomogeneous source wave, the homogeneous and reflected waves at the sum frequency and the interface normal are all lie in the

$xz$ -plane. Since the propagation of inhomogeneous wave,  $\exp i\{(\bar{k}_1^t + \bar{k}_2^t) \cdot \bar{r} - (\mathbf{w}_1 + \mathbf{w}_2)t\}$  is proportional to  $P^{NLS}(\mathbf{w}_3)$ . Its angle with the face normal  $\mathbf{q}_3^s$  is determined by

$$\sin \mathbf{q}_3^s = \left| k_{1x}^t + k_{2x}^t \right| / \left| \bar{k}_1^t + \bar{k}_2^t \right|. \quad (2.17)$$

The wave vectors  $\bar{k}_1^t$  and  $\bar{k}_2^t$  can be obtained by Snell's law for refraction as in the linear case. Making use of trigonometric relations, one can find

$$\begin{aligned} |k_3^T|^2 \sin^2 \mathbf{q}_3^T &= |k_3^R|^2 \sin^2 \mathbf{q}_3^R \\ &= |k_1^i|^2 \sin^2 \mathbf{q}_1^i + |k_2^i|^2 \sin^2 \mathbf{q}_2^i \\ &\quad + 2|k_1^i||k_2^i| \sin \mathbf{q}_1^i \sin \mathbf{q}_2^i \cos \mathbf{j}. \end{aligned} \quad (2.18)$$

By substituting the magnitude of wave vector  $k = \frac{\mathbf{w}}{c} \sqrt{\mathbf{e}}$ , equation (2.18) can be rewritten as

$$\begin{aligned} \mathbf{e}_3^T \mathbf{w}_3^2 \sin^2 \mathbf{q}_3^T &= \mathbf{e}_3^R \mathbf{w}_3^2 \sin^2 \mathbf{q}_3^R \\ &= \mathbf{e}_1^R \mathbf{w}_1^2 \sin^2 \mathbf{q}_1^i + \mathbf{e}_2^R \mathbf{w}_2^2 \sin^2 \mathbf{q}_2^i \\ &\quad + 2\sqrt{\mathbf{e}_1^R \mathbf{e}_2^R} \mathbf{w}_1 \mathbf{w}_2 \sin \mathbf{q}_1^i \sin \mathbf{q}_2^i \cos \mathbf{j}. \end{aligned} \quad (2.19)$$

In the special case that the planes of incidence coincide ( $\mathbf{j} = 0$ ), a relationship will become as,

$$\sqrt{\mathbf{e}_3^T} \sin \mathbf{q}_3^T = \sqrt{\mathbf{e}_3^R} \sin \mathbf{q}_3^R = \sqrt{\mathbf{e}_1^R} \sin \mathbf{q}_1^i. \quad (2.20)$$

Another conditions so that conserved tangential momentum components exists in equation (2.15) is

$$\bar{k}_3^T \sin \mathbf{q}_3^T = \bar{k}_3^s \sin \mathbf{q}_3^s = k_3^R \sin \mathbf{q}_3^R, \quad (2.21)$$

or, alternatively,

$$\mathbf{e}_3^T \sin^2 \mathbf{q}_3^T = \mathbf{e}_3^s \sin^2 \mathbf{q}_3^s = \mathbf{e}_3^R \sin^2 \mathbf{q}_3^R. \quad (2.22)$$

Finally, we get

$$\sqrt{\mathbf{e}_1^R} \sin \mathbf{q}_1^i = \sqrt{\mathbf{e}_3^R} \sin \mathbf{q}_3^R = \sqrt{\mathbf{e}_3^T} \sin \mathbf{q}_3^T = \sqrt{\mathbf{e}_3^s} \sin \mathbf{q}_3^s, \quad (2.23)$$

or, equivalently, in terms of refractive index by,

$$n_1^R \sin \mathbf{q}_1^i = n_3^R \sin \mathbf{q}_3^R = n_3^T \sin \mathbf{q}_3^T = n_3^s \sin \mathbf{q}_3^s. \quad (2.24)$$

These are known as general laws of reflection and refraction.

### 2.2.3 Polarization and intensity of the reflected second-harmonic wave

The calculations of the polarization and intensity of the reflected wave at the sum frequency  $\mathbf{w}_3 = \mathbf{w}_1 + \mathbf{w}_2$  is presented in this section. We restrict our attention to the reflected wave at  $\mathbf{w}_3$  with the electric field vector parallel to the plane of incidence, for second-harmonic generation where  $\mathbf{w}_1 = \mathbf{w}_2 = \mathbf{w}$ . Therefore,  $\mathbf{w}_3 = 2\mathbf{w}$ . This second-harmonic wave is created by the  $x$  and  $z$  components of nonlinear polarization ( $P_y^{NLS}(2\mathbf{w}) = 0 = E_y(2\mathbf{w})$ ). Let  $P_{//}^{NLS}$  denote the magnitude of the nonlinear polarization in the plane of reflection,  $\mathbf{a}$  be the angle between the propagation direction of the source  $\bar{k}^s$  and the direction of nonlinear polarization as illustrated in Figure 2.5.

The continuity of tangential components of electric  $\vec{E}$  and magnetic  $\vec{H}$  field is required for the calculation of the amplitude of the reflected second-harmonic wave. As evident from the solution of Maxwell's equations for nonlinear medium, one can find



$$E_{//}^R = \frac{4\mathbf{p}_{//}^{NLS} \sin \mathbf{a}}{\sqrt{\mathbf{e}_R} \cos \mathbf{q}_T + \sqrt{\mathbf{e}_T} \cos \mathbf{q}_R} \left[ \frac{1 - (\mathbf{e}_s^{-1} + \mathbf{e}_T^{-1}) \mathbf{e}_R \sin^2 \mathbf{q}_R}{\sqrt{\mathbf{e}_s} \cos \mathbf{q}_T + \sqrt{\mathbf{e}_T} \cos \mathbf{q}_s} \right] + \frac{4\mathbf{p}_{//}^{NLS} \cos \mathbf{a} \sin \mathbf{q}_s}{\sqrt{\mathbf{e}_T \mathbf{e}_s} \cos \mathbf{q}_T + \mathbf{e}_T \cos \mathbf{q}_R}. \quad (2.27)$$

Applying equation (2.23), the reflected second-harmonic amplitude can be rewritten as

$$E_{//}^R = \frac{4\mathbf{p}_{//}^{NLS} \sin \mathbf{q}_s \sin^2 \mathbf{q}_T \sin(\mathbf{a} + \mathbf{q}_T + \mathbf{q}_s)}{\mathbf{e}_R (2\mathbf{w}) \sin \mathbf{q}_R \sin(\mathbf{q}_T + \mathbf{q}_R) \cos(\mathbf{q}_T - \mathbf{q}_R) \sin(\mathbf{q}_T + \mathbf{q}_s)}, \quad (2.28)$$

or

$$E_{//}^R = 4\mathbf{p}_{//}^{NLS} F_{R, //}^{NL}, \quad (2.29)$$

where

$$F_{R, //}^{NL} = \frac{\sin \mathbf{q}_s \sin^2 \mathbf{q}_T \sin(\mathbf{a} + \mathbf{q}_T + \mathbf{q}_s)}{\mathbf{e}_R (2\mathbf{w}) \sin \mathbf{q}_R \sin(\mathbf{q}_T + \mathbf{q}_R) \cos(\mathbf{q}_T - \mathbf{q}_R) \sin(\mathbf{q}_T + \mathbf{q}_s)}. \quad (2.30)$$

The intensity of reflected second-harmonic wave is given by the real part of Poynting vector times the cross-section area  $A_R$  :

$$I_R(2\mathbf{w}) = \frac{c}{8\mathbf{p}} \sqrt{\mathbf{e}_R} |E_{//}^R(2\mathbf{w})|^2 A_R, \quad (2.31)$$

where  $A_R = dd' \cos \mathbf{q}_R / \cos \mathbf{q}_i$  and  $dd'$  is the area of the rectangular slit which defines the beam profile of the incident laser.

## 2.2.4 Second-harmonic generation at total reflection

The total reflection phenomenon of second-harmonic wave, included in the theory of Bloembergen and Pershan (1962), was experimentally observed for the first time by Bloembergen and Lee (1967) and later by Bloembergen, Simon, and Lee

(1969). This phenomenon remains the same as for linear case it can occur when the light incidents from a optically denser linear medium to nonlinear medium of lower refractive index. The geometrical situation just before total reflection of second-harmonic wave occurs is shown in Figure 2.6. The transmitted fundamental beam  $\bar{k}^t(\mathbf{w})$ , goes in same direction as induced nonlinear polarization wave  $\bar{k}^s$ , the homogeneous transmitted wave  $\bar{k}^T$  goes in somewhere different direction. The effect of dispersion causes the reflected fundamental wave  $\bar{k}^r(\mathbf{w})$  goes in a different direction with the reflected second-harmonic wave. There are two transmitted harmonic beams in nonlinear medium possessing the birefringence. As the angle of incident  $\mathbf{q}_i$  increases both beam with wave vectors  $\bar{k}^s$  and  $\bar{k}^t$  will disappear simultaneously, while the transmitted harmonic wave will still remain. For large angle of incidence only the reflected harmonic beam persists. The angle of harmonic reflection  $\mathbf{q}_R$ , transmission source  $\mathbf{q}_s$ , and homogeneous harmonic transmission  $\mathbf{q}_T$  are related by generalized Snell's law

$$n_{liq}(\mathbf{w}) \sin \mathbf{q}_i = n_{liq}(2\mathbf{w}) \sin \mathbf{q}_R = n(\mathbf{w}) \sin \mathbf{q}_S = n(2\mathbf{w}) \sin \mathbf{q}_T. \quad (2.32)$$

The indices of refraction are corresponded to the dielectric constants in the notation of Bloembergen and Pershan theory (equation. 2.23) by  $\sqrt{\mathbf{e}_R} = n_{liq}(2\mathbf{w})$ ,  $\sqrt{\mathbf{e}_s} = n(\mathbf{w})$ , and  $\sqrt{\mathbf{e}_T} = n(2\mathbf{w})$ . The indices without subscripts refer to the ADP crystal. The critical angles for total reflection of the transmitted source and transmitted homogeneous wave are given by

$$\mathbf{q}_{cr}(\mathbf{w}) = \sin^{-1} \left( n(\mathbf{w}) / n_{liq}(\mathbf{w}) \right) \quad (2.33)$$

and



$$\begin{bmatrix} P_x^{NLS}(2\mathbf{w}) \\ P_y^{NLS}(2\mathbf{w}) \\ P_z^{NLS}(2\mathbf{w}) \end{bmatrix} = \begin{bmatrix} 0 & 0 & 0 & \mathbf{c}_{14} & 0 & 0 \\ 0 & 0 & 0 & 0 & \mathbf{c}_{14} & 0 \\ 0 & 0 & 0 & 0 & 0 & \mathbf{c}_{36} \end{bmatrix} \begin{bmatrix} E_x^2(\mathbf{w}) \\ E_y^2(\mathbf{w}) \\ E_z^2(\mathbf{w}) \\ 2E_y(\mathbf{w})E_z(\mathbf{w}) \\ 2E_x(\mathbf{w})E_z(\mathbf{w}) \\ 2E_x(\mathbf{w})E_y(\mathbf{w}) \end{bmatrix} \quad (2.35)$$

Assume that the fundamental field is polarized perpendicular to the plane of incidence or is polarized among the  $x$  and  $-y$  directions with respect to the crystallographic axes of the ADP. In this case the nonlinear source inside the crystal will be along the  $z$  direction and its amplitude is given in terms of the transmitted fundamental field components by

$$P_z^{NLS}(2\mathbf{w}) = \mathbf{c}_{36}^{NL} E_x^T(\mathbf{w})E_y^T(\mathbf{w}), \quad (2.36)$$

where  $\mathbf{c}_{36}^{NL}$  is the nonlinear susceptibility of ADP crystal which give rise to a polarization at the harmonic frequencies. The amplitude of nonlinear polarization  $P_z^{NLS}(2\mathbf{w})$  can be expressed in terms of the amplitude  $E_o$  of the incident fundamental wave by

$$P_z^{NLS}(2\mathbf{w}) = \mathbf{c}_{36}^{NL} \mathbf{h} (F_T^L E_o)^2, \quad (2.37)$$

where  $\mathbf{h}$  is the geometrical factor, which depends on the orientation of the fundamental vector and the nonlinear polarization component with respect to the crystallographic axis of the nonlinear crystal. The linear Fresnel factor  $F_T^L$  describes the change in amplitude of the fundamental wave on the transmission wave. In case of the laser polarization perpendicular to the plane of incident it is

$$F_T^L = \frac{2 \cos \mathbf{q}_i}{\cos \mathbf{q}_i + \sin \mathbf{q}_{cr}(\mathbf{w}) \cos \mathbf{q}_s}. \quad (2.38)$$

The electric field amplitude of reflected second-harmonic wave is given by

$$E_R(2\mathbf{w}) = 4\mathbf{p} P^{NLS} F_{R, //}^{NL}. \quad (2.39)$$

For the case of nonlinear polarization parallel to the plane of incident, the nonlinear Fresnel factor  $F_{R, //}^{NL}$ , according to the Bloembergen and Pershan theory is given by

$$F_{R, //}^{NL} = \frac{\sin \mathbf{q}_S \sin^2 \mathbf{q}_T \sin(\mathbf{a} + \mathbf{q}_T + \mathbf{q}_S)}{\mathbf{e}_R(2\mathbf{w}) \sin \mathbf{q}_R \sin(\mathbf{q}_T + \mathbf{q}_R) \cos(\mathbf{q}_T - \mathbf{q}_R) \sin(\mathbf{q}_T + \mathbf{q}_S)}. \quad (2.30)$$

Here  $\mathbf{a}$  is the angle between the nonlinear polarization in the plane of incidence and direction of source vector  $k_S$ .

The intensity of reflected harmonic wave is

$$I_R(2\mathbf{w}) = \frac{c}{8\mathbf{p}} \mathbf{e}_R^{1/2} |E_o|^4 dd' (4\mathbf{p} \mathbf{c}_{36}^{NL})^2 \mathbf{h}^2 |F_T^L|^4 |F_R^{NL}|^2 \cos \mathbf{q}_R (\cos \mathbf{q}_i)^{-1}, \quad (2.40)$$

where  $dd' \cos \mathbf{q}_R / \cos \mathbf{q}_i$  is the area of incident laser beam profile. Since

$\frac{c}{8\mathbf{p}} \mathbf{e}_R^{1/2} |E_o|^4 dd' (4\mathbf{p} \mathbf{c}_{36}^{NL})^2 \mathbf{h}^2$  is constant, we can write  $I_R(2\mathbf{w})$  in relative units as

$$I_R(2\mathbf{w}) \propto |F_T^L|^4 |F_R^{NL}|^2 \cos \mathbf{q}_R (\cos \mathbf{q}_i)^{-1}. \quad (2.41)$$

In the study, ADP crystal is the negative ( $n_e < n_o$ ) uniaxial crystal and its extraordinary refractive index  $n_e^{2w}(\mathbf{q})$  depends on the angle  $\mathbf{q}$  between the propagation direction and the crystal optic axis. The value of  $n_e^{2w}(\mathbf{q})$  can be obtained from the equation of the index ellipsoid as

$$\frac{1}{[n_e^{2w}(\mathbf{q})]^2} = \frac{\cos^2(\mathbf{q})}{[n_o^{2w}]^2} + \frac{\sin^2(\mathbf{q})}{[n_e^{2w}(\mathbf{p}/2)]^2}. \quad (2.42)$$

$n_o^w$  and  $n_e^w$  are the ordinary and extraordinary refractive indices for the laser light and  $n_o^{2w}$  and  $n_e^{2w}(\mathbf{q})$  are the corresponding quantities for the second-harmonic frequency.

### 2.2.5 Phase-matching in second-harmonic generation

According to the out put intensity of second-harmonic generation, which is proportional to the phase factor (Yariv, 1991):

$$I(2\mathbf{w}) \propto |E_0|^4 \frac{\sin^2(\Delta kl/2)}{(\Delta kl/2)^2}, \quad (2.43)$$

with  $l$  being the optical path length. The crucial parameter that controls the intensity of the second-harmonic generation is  $\Delta k$ , which is given by,

$$\Delta k = k^{(2w)} - 2k^{(w)}, \quad (2.44)$$

where  $k^{(w)} = n(\mathbf{w}) \frac{\mathbf{w}}{c}$  is the wave vector of fundamental beam and  $k^{(2w)} = n(2\mathbf{w}) \frac{2\mathbf{w}}{c}$

is the second-harmonic wave vector. When the condition  $\Delta k = 0$  is achieved, the interaction that leads to second-harmonic generation is said to be phase-matched (Maker et. al., 1962; Goidmaine, 1962). For dielectric material, the dielectric constant always proportional to the frequency, so it cannot achieve phase-matching. However, for birefringence crystals such as KDP, ADP, and RDP, it is possible to achieve phase-matching, since there is the ordinary wave with index of refraction  $n_o$  and the extraordinary wave with index of refraction  $n_e(\mathbf{q})$  that depend on the angle  $\mathbf{q}$  between direction of propagation and the optic axis. Let  $\mathbf{q}_m$  be the angle between the optic axis and the direction of wave propagation which phase-matching is achieved ( $\Delta k = 0$ , or  $n_e^{(2w)}(\mathbf{q}_m) = n_o^{(w)}$ ). Therefore if the fundamental beam is launched along

$\mathbf{q}_m$  as an ordinary ray, the second-harmonic beam will be generated along the same direction as extraordinary ray. The situation is illustrated by Figure 2.7.

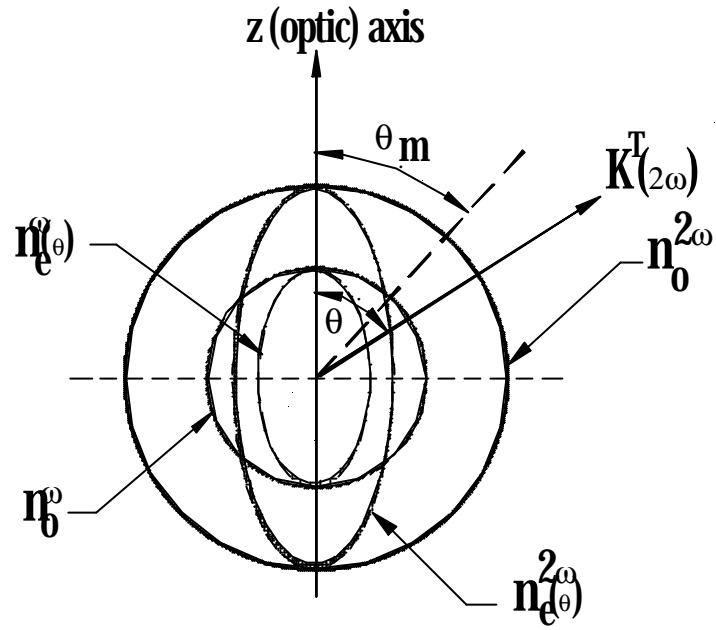


Figure 2.7. The refractive index for ordinary and extraordinary rays in a negative uniaxial crystal. The condition of phase-matching is satisfied at  $\mathbf{q}_m$ .

The angle  $\mathbf{q}_m$  where  $n_e^{(2w)}(\mathbf{q}_m) = n_o^{(w)}$  can be obtained by

$$\frac{1}{[n_e^{2w}(\mathbf{q})]^2} = \frac{\cos^2(\mathbf{q}_m)}{[n_o^{2w}]^2} + \frac{\sin^2(\mathbf{q}_m)}{[n_e^{2w}(\mathbf{p}/2)]^2} = \frac{1}{[n_o^w]^2}, \quad (2.45)$$

Solving for  $\mathbf{q}_m$ , we get

$$\mathbf{q}_m = \sin^{-1} \frac{\hat{\mathbf{e}} \cdot (\mathbf{n}_o^w)^{-2} - (\mathbf{n}_o^{2w})^{-2}}{\hat{\mathbf{e}} \cdot (\mathbf{n}_e^{2w}(\mathbf{p}/2))^{-2} - (\mathbf{n}_o^{2w})^{-2}} \hat{\mathbf{u}}^{1/2} \quad (2.46)$$

Normally, the phase-matched second-harmonic generation can be performed in transmission geometry (Giordmaine, 1962; Maker, Terhune, Nissenoff, and Savage, 1965; Boyd, Askin, Dziedzic, and Kleinman, 1965; Bhanthumnavin and Lee, 1994). In fact, phase-matched second-harmonic can be observed in reflection geometry as well (Bloembergen and Lee, 1967; Lee and Bhanthumnavin, 1976; Bhanthumnavin and Lee, 1994).

### 2.2.6 Nonlinear Brewster angle

For the nonlinear crystal of  $\bar{4}2m$  point group, such as ADP, KDP and RDP, when the incident laser beam is polarized with the electric field  $E_o$  perpendicular to the plane of incident, the nonlinear polarization is parallel to the optic axis of crystal ( $z$  – axis). The reflected second-harmonic will lie in the plane of incidence. At the nonlinear Brewster angle, the reflected second-harmonic wave completely vanishes. This phenomenon was theoretically predicted by Bloembergen and Pershan (1962) and was firstly observed by Chang and Bloembergen (1966) in GaAs, Lee and Bhanthumnavin (1976) in KDP and was theoretically predicted in ADP by Bhanthumnavin and Ampole (1990). The physical interpretation of nonlinear Brewster's angle is shown in Figure 2.8.

When the angle of incidence reaches the nonlinear Brewster angle, the fundamental beam will induce a nonlinear polarization inside the medium in direction of the reflected second-harmonic ray. According to the classical dipole radiation theory, the polarization cannot radiate in this direction. Therefore the intensity of reflected harmonic wave must vanish,

$$I^R(2\omega) = 0. \quad (2.47)$$

It is clear that  $I^R(2\omega)$  is zero when the nonlinear Fresnel factor  $F_{R,II}^{NL}$  equals to zero,

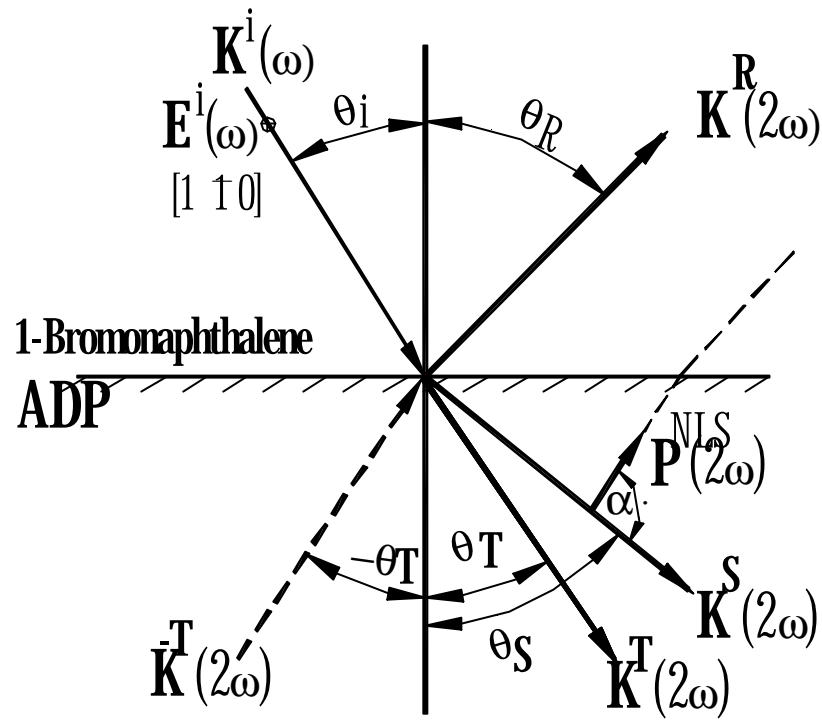


Figure 2.8. The physical interpretation of nonlinear Brewster angle.

which leads to

$$\sin(\mathbf{a} + \mathbf{q}_s + \mathbf{q}_T) = 0 \quad (2.48)$$

or

$$\mathbf{a} + \mathbf{q}_s + \mathbf{q}_T = 0, \mathbf{p}, 2\mathbf{p}, \dots \quad (2.49)$$

## Chapter III

### Procedure

#### 3.1 Introduction

In the study, the ultrashort pulse laser at  $\lambda = 900$  nm is utilized as a fundamental beam in order to generate the second-harmonic light beam from the ADP crystal. The polarization of this fundamental field is set to be perpendicular with the plane of incidence or in  $[1 \bar{1} 0]$  direction with respect to the crystallographic axes of the ADP crystal. Under this situation, the nonlinear polarization that is the source of second-harmonic field will be induced along the optic axes of the crystal or in  $[0 0 1]$  direction as indicated in Figure 3.1.

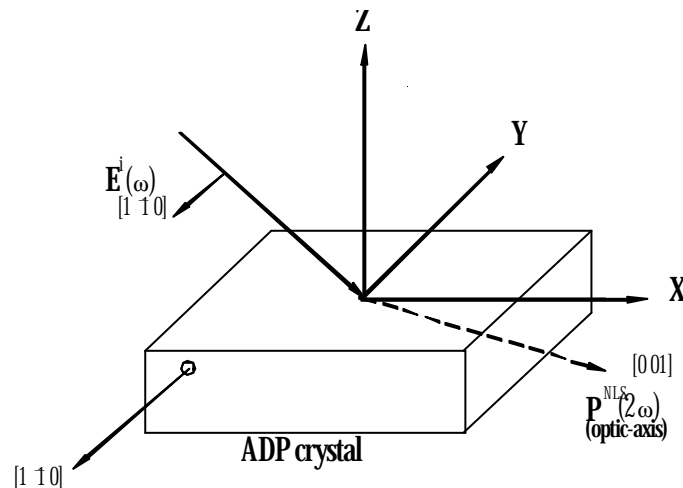


Figure 3.1. Geometry illustrates the crystallographic axes system ( $x, y, z$ )

The study of nonlinear Brewster angle phenomenon or the vanishing of the p-polarized second-harmonic intensity in reflection at particular angle of incidence can be done by using the crystal orientation as shown in Figure 3.1. The theory of Bloembergen and Pershan given in previous chapter is employed for the theoretical calculation of the relative reflected second-harmonic intensity. Before calculating second-harmonic intensity (SHI) in reflection, involved parameters need to be known. Therefore, this chapter is about some properties and quantities of parameters involved in the theoretical study of reflected second-harmonic generation. Furthermore, the algorithm of theoretical calculation of reflected second harmonic intensity by program C++ is also described.

### 3.2 Ultrashort pulse laser

As ultrashort laser pulse is utilized as the fundamental field in order to induce the nonlinear polarization  $P^{NLS}(2\mathbf{w})$  that acts as the source of optical second-harmonic field. According to the intensity of reflected second harmonic as described in previous chapter, it is clear that the high intensity of second-harmonic depends on the fourth power of the applied fundamental electric field,  $E_0(\mathbf{w})$ . Therefore, the ultrashort pulse laser is suitable to be used in the study because its peak power is rather high ( $\geq 1$  MW) and its energy is relatively small ( $\sim 1$  nJ) and can be concentrated in a very short temporal interval ( $\sim 10^{-15}$  s). Due to high peak power pulse and small energy, the crystal can tolerate the excitation without damage.

### 3.3 ADP crystal

The nonlinear crystal used in our study is ammonium dihydrogen phosphate (ADP). ADP is a crystal of the  $\bar{4}2m$  point group as mentioned in section 2.2.4. The transparency range of ADP crystal is 184-1500 nm, so that the fundamental (900nm) and the second harmonic (450 nm) waves can not be absorbed in the crystal. The crystal is suitable for the study, because its surface damage threshold is very high. Moreover, its linear index of reflection is relatively low. Therefore it will allow us to perform phase matched second harmonic generation at total reflection via 1-bromonaphthalene which has larger indices of reflection than the crystal at both the fundamental and second harmonic frequency. The refractive indices of the ADP crystal at the fundamental wavelength of 900 nm measured by Zernike (1964) are

$$n_o^w = 1.5120,$$

$$n_e^w(p/2) = 1.4709.$$

The refractive indices of ADP at the second harmonic wavelength of 450 nm can be obtained by the dispersion relations (Dmitriev, Gurzadyan and Nikogosyan, 1991)

$$(n_o)^2 = 2.302842 + \frac{0.011125165}{I^2 - 0.013253659} + \frac{15.102464I^2}{I^2 - 400},$$

$$(n_e(p/2))^2 = 2.163510 + \frac{0.009616676}{I^2 - 0.01298912} + \frac{5.919896I^2}{I^2 - 400},$$

where the unit of the wavelength  $\lambda$  is in  $\mu\text{m}$ . Substituting the second harmonic wave length of  $\lambda = 0.450 \mu\text{m}$  yields

$$n_o^{2w} = 1.53426,$$

$$n_e^{2w}(p/2) = 1.4870.$$

Now the phase-matching angle given in equation (2.46) can be evaluated as

$$\begin{aligned}
 \theta_m &= \sin^{-1} \left[ \frac{(n_o^w)^{-2} - (n_o^{2w})^{-2}}{(n_e^{2w}(\theta/2))^{-2} - (n_o^{2w})^{-2}} \right]^{1/2} \\
 &= \sin^{-1} \left[ \frac{(1.5120)^{-2} - (1.53426)^{-2}}{(1.4870)^{-2} - (1.53426)^{-2}} \right]^{1/2} \\
 &= 42.68^\circ.
 \end{aligned}$$

### 3.4 Liquid 1-bromonaphthalene

In order to achieve the occurrence of total reflection of the second harmonic beam, the optically denser fluid 1-bromonaphthalene, whose indices of refraction is higher than the crystal at both the fundamental and second harmonic frequency, is the proper choice of the linear medium. The fluid has transparency range at 400-1600 nm (Bhanthumnavin and Lee, 1994), therefore the absorption of the reflected wave at both fundamental and second harmonic frequency will occur. Furthermore, since the chemical property of 1-bromonaphthalene is relative inertness, it is good for practical study, because of the deterioration of ADP crystal by electrochemical process will not occur. Interpolating by means of the Cauchy dispersion relation (Jenkins and White, 1976) as shown in the Appendix A gives

$$\begin{aligned}
 n_{liq}(\mathbf{w}) &= 1.6335 \\
 n_{liq}(2\mathbf{w}) &= 1.6952.
 \end{aligned}$$

### 3.5 Computation of Relative Reflected Second-harmonic Intensity by using C++ Program

The theoretical calculation of reflected second harmonic intensity based on Bloembergen and Pershan theory (1962) was performed by C++ version 3. The results

were stored in text file and then plotted by using Microsoft Excel version 7. The steps of evaluation are indicated in Figure 3.2. Although the reflected second harmonic intensity is as a function of incident angle  $q_i$ , the step starts with the assigning of transmitted angle  $q_t$  as input instead of  $q_i$ .

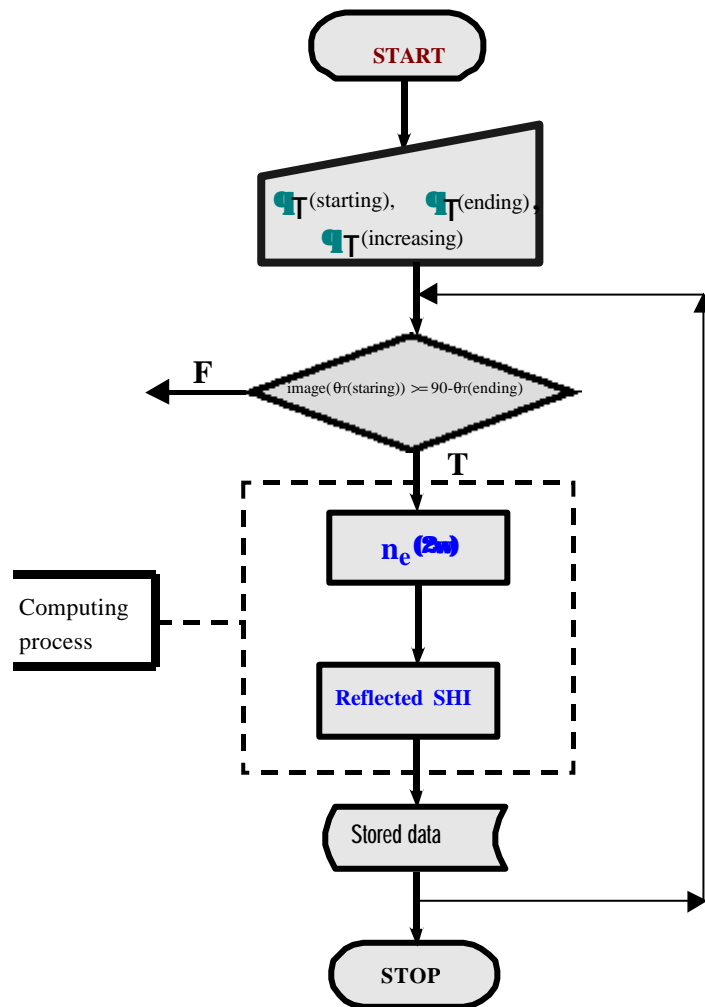


Figure 3.2. Flowchart for theoretical calculation of SHI in reflection

As depicted in Figure 3.2 the calculation procedure consists of two major steps as follows



Here  $\mathbf{g}$  is the angle between optic axis ( $P^{NLS}(2\mathbf{w})$ ) of the crystal and the incident surface, which depends on the crystallographic cut of the crystal. Thus the value of  $n_e^{2w}(\mathbf{q})$  at any  $\mathbf{q}$  can be written in terms of the angle of transmission  $\mathbf{q}_T$  as

$$n_e^{2w}(90^\circ - \mathbf{g} + \mathbf{q}_T) = \sqrt{\frac{1}{\frac{\cos^2(90^\circ - \mathbf{g} + \mathbf{q}_T)}{(n_o^{2w})^2} + \frac{\sin^2(90^\circ - \mathbf{g} + \mathbf{q}_T)}{(n_e^{2w}(\theta/2))^2}}}. \quad (3.3)$$

The angle  $\mathbf{g}$  can be easily known when the nonlinear crystal was assigned and the orientation of  $P^{NLS}(2\mathbf{w})$  was known.

### 3.5.2 The calculation of relative reflected second-harmonic intensity

#### (SHI)

After calculating  $n_e^{2w}(\mathbf{q})$ , it is now time to obtain the values of  $\mathbf{q}_i$ ,  $\mathbf{q}_R$  and  $\mathbf{q}_s$

via generalized Snell's law by

$$\begin{aligned} \mathbf{q}_i &= \sin^{-1} \left( \frac{n_e^{2w}(\mathbf{q}) \sin \mathbf{q}_T}{n_{liq}^w} \right) \\ \mathbf{q}_R &= \sin^{-1} \left( \frac{n_{liq}^w \sin \mathbf{q}_i}{n_{liq}^{2w}} \right) \end{aligned} \quad (3.4)$$

and

$$\mathbf{q}_s = \sin^{-1} \left( \frac{n_{liq}^w \sin \mathbf{q}_i}{n_o^w} \right)$$

The relative magnitude of reflected SHI depends on  $F_T^L$ , and  $F_{R, //}^{NL}$  as

$$I_R(2\mathbf{w}) \cong |F_T^L|^4 |F_{R, //}^{NL}|^2 \cos \mathbf{q}_R (\cos \mathbf{q}_i)^{-1},$$

as shown in Figure 3.4, since the factor

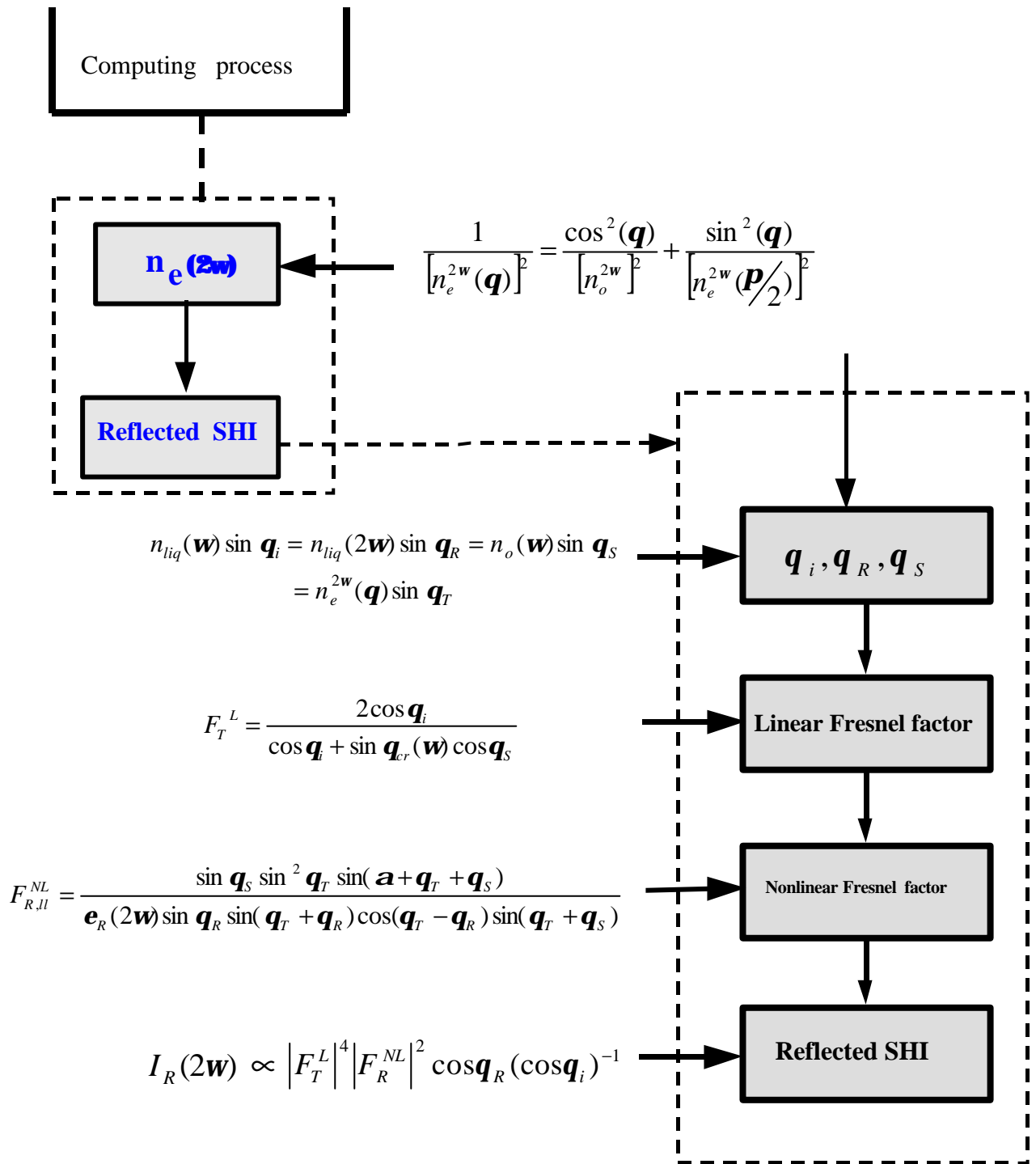


Figure 3.4. Process for computing of SHI in reflection

$$F_{R, //}^{NL} = \frac{\sin \mathbf{q}_S \sin^2 \mathbf{q}_T \sin(\mathbf{a} + \mathbf{q}_T + \mathbf{q}_S)}{\mathbf{e}_R(2\mathbf{w}) \sin \mathbf{q}_R \sin(\mathbf{q}_T + \mathbf{q}_R) \cos(\mathbf{q}_T - \mathbf{q}_R) \sin(\mathbf{q}_T + \mathbf{q}_S)} \quad (2.30)$$

depends on the crystallographic cut of the crystal. According to the geometry used in the study (see figure 3.3) it is clear that

$$\mathbf{a} + \mathbf{q}_S = 270^\circ + \mathbf{g}, \quad (3.5)$$

because  $\mathbf{a} + \mathbf{q}_S$  is the angle between the face normal direction and the optic axis. Thus the factor  $F_{R, //}^{NL}$  can be rewritten as

$$F_{R, //}^{NL} = \frac{\sin \mathbf{q}_S \sin^2 \mathbf{q}_T \sin(270^\circ + \mathbf{g} + \mathbf{q}_T)}{\sin \mathbf{q}_R \sin(\mathbf{q}_T + \mathbf{q}_R) \cos(\mathbf{q}_T - \mathbf{q}_R) \sin(\mathbf{q}_T + \mathbf{q}_S)}. \quad (3.6)$$

Here the term of  $\mathbf{e}_R(2\mathbf{w})$  has been taken as a constant.

The detail of computer program C<sup>++</sup> is available in the Appendix B. The program used to calculate the reflected SHI in previous work of Bhanthumnavin and Lee (1994). The simulated results are exactly correct to those previous results. This means that the program is acceptable be use of the thesis.

# Chapter IV

## Results and Discussions

### 4.1 Introduction

In this chapter the results from theoretical investigation of SHI in reflection from ADP crystal using ultrashort laser pulse of 900nm as an excitation source are analyzed and explained. It is shown that this study agrees well to the hypothesis, especially for the prediction of nonlinear Brewster angles.

### 4.2 Phase-matched Second-harmonic Generation

The reflected second-harmonic generation, under phase matching at total reflection has been theoretically described in chapter 2. In our study, ADP is set up with its optic axis inclining at  $\mathbf{q}_m = 42.68^\circ$  (see for calculation in sec. 3.3) from the incident surface, in order to facilitate a phase matching condition. At the critical angle, the harmonic waves vector  $k^s$  and  $k^T$  go in same direction along the interface, This situation leads to the enhancement of the reflected second-harmonic intensity, as evidence from the nonlinear Fresnel Factor

$$F_{R, //}^{NL} = \frac{\sin \mathbf{q}_S \sin^2 \mathbf{q}_T \sin(\mathbf{a} + \mathbf{q}_T + \mathbf{q}_S)}{\mathbf{e}_R(2\mathbf{w}) \sin \mathbf{q}_R \sin(\mathbf{q}_T + \mathbf{q}_R) \cos(\mathbf{q}_T - \mathbf{q}_R) \sin(\mathbf{q}_T + \mathbf{q}_S)}. \quad (2.30)$$

When  $\mathbf{q}_T = \mathbf{q}_S = 90^\circ$ , then

$$F_{R, //}^{NLS} \rightarrow \infty .$$

Also for reflected second-harmonic intensity,

$$I_R(2\mathbf{w}) \rightarrow \infty.$$

Simulation by varying the angle of incidence  $\mathbf{q}_i$  from  $55^\circ$ - $75^\circ$  is provided in Figure 4.1. Figure 4.1 shows that the intensity increases nearly at eight orders of magnitude at critical angle

$$\begin{aligned} \mathbf{q}_i &= \mathbf{q}_{cr}(\mathbf{w}) = \mathbf{q}_{cr}(2\mathbf{w}) \\ &= \sin^{-1} \left[ \frac{n_o^w \sin 90^\circ}{n_{liq}^w} \right] \\ &= \sin^{-1} \left[ \frac{1.5120}{1.6335} \right] = 67.76^\circ. \end{aligned}$$

Comparing these results with previous work of Bhanthumnavin and Lee (1990,1994), finds that both of them are alike. In addition, the theoretical result agrees well with the prediction of Bloembergen and Pershan(1962). Because the nonlinear crystals used in the previous works carry the same point-group as those in this study, one can deduce that under the new proposed crystallographic orientation, the phase-matched second-harmonic generation at total reflection can be achieved as proposed.

### 4.3 Nonlinear Brewster angle

According to the nonlinear Brewster angle condition, the reflected second-harmonic intensity will go to zero:

$$I_R(2\mathbf{w}) = 0.$$

The condition for this situation is:

$$F_{R, //}^{NL} = \frac{\sin \mathbf{q}_s \sin^2 \mathbf{q}_r \sin(\mathbf{a} + \mathbf{q}_T + \mathbf{q}_S)}{\mathbf{e}_R(2\mathbf{w}) \sin \mathbf{q}_R \sin(\mathbf{q}_T + \mathbf{q}_R) \cos(\mathbf{q}_T - \mathbf{q}_R) \sin(\mathbf{q}_T + \mathbf{q}_S)} = 0,$$

or

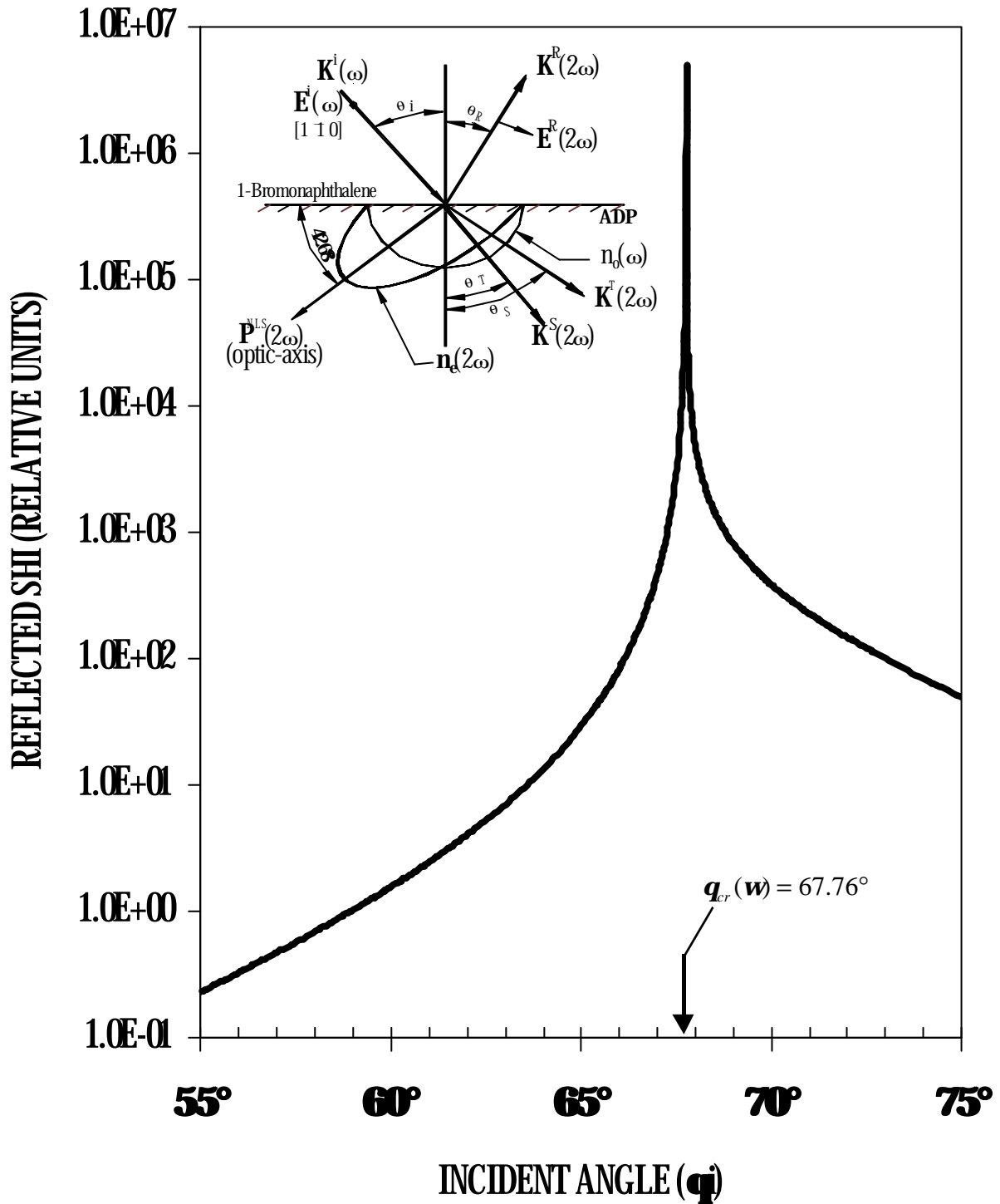


Figure 4.1 Relative reflected second-harmonic intensity (SHI) from ADP crystal as a function of  $q_i$  with phase-matching at total reflection.  $q_i = q_{cr}(w) = q_{cr}(2w) = 67.76^\circ$

$$\mathbf{a} + \mathbf{q}_s + \mathbf{q}_r = n\mathbf{p}, \quad n = 0, 1, 2, \dots$$

This leads to the fact that nonlinear Brewster angle is not unique for a crystal but depends on the orientation of  $P^{NLS}(2\mathbf{w})$  inside the crystal. In the study several orientation of  $P^{NLS}(2\mathbf{w})$  of ADP were studied and the results will now be presented.

#### 4.3.1 Nonlinear Brewster angle of ADP with $P^{NLS}(2\mathbf{w})$ making an angle $42.68^\circ$ from the incident surface

In this case, the crystallographic cut of ADP is same as the case of phase matching condition, so the condition for nonlinear Brewster angle is

$$\mathbf{a} + \mathbf{q}_s + \mathbf{q}_r = 2\mathbf{p}.$$

Here  $\mathbf{a} + \mathbf{q}_s$  is the angle between the face normal and  $P^{NLS}(2\mathbf{w})$  direction and may be taken as the fixed angle, as show in the inset of Figure 4.2

$$\mathbf{a} + \mathbf{q}_s = 270^\circ + 42.68^\circ = 312.68^\circ.$$

Thus the angle of transmission  $\mathbf{q}_r$  is easily to known,

$$\mathbf{q}_r = 360^\circ - 312.68^\circ = 47.32^\circ.$$

The incident angle or nonlinear Brewster angle, which gives,  $\mathbf{q}_f = 47.32^\circ$  can be found by Snell's law as

$$n_{liq}(\mathbf{w}) \sin \mathbf{q}_f^{NB} = n_e^{2w}(2\mathbf{q}_r) \sin \mathbf{q}_r.$$

$$\begin{aligned} \text{Thus } \mathbf{q}_f^{NB} &= \sin^{-1} \left[ \frac{n_e^{2w}(94.64^\circ) \sin 47.32^\circ}{n_{liq}(\mathbf{w})} \right] \\ &= \sin^{-1} \left[ \frac{1.4873 \sin 47.32^\circ}{1.6335} \right] \\ &= 42.02^\circ. \end{aligned}$$

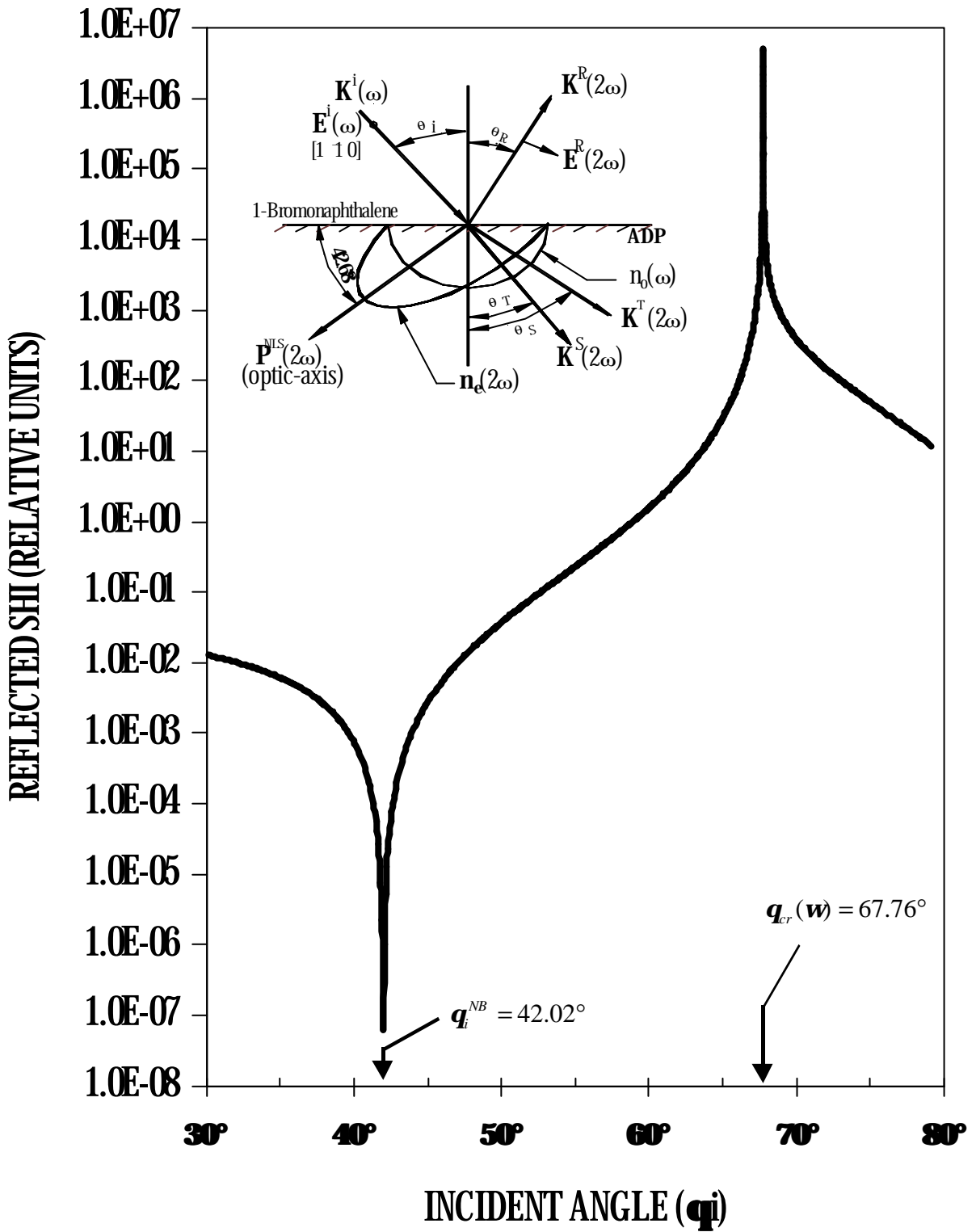


Figure 4.2. Relative reflected second-harmonic intensity (SHI) from ADP crystal as a function of  $q_i$ . Nonlinear Brewster angle is at  $q_i^{NB} = 42.02^\circ$  with  $P^{NLS}(2w)$  is at  $42.68^\circ$  from the incident surface.

The variation of optical second-harmonic intensity in reflection is given by figure 4.2. The graph shows that achievement of both maximum and minimum intensity of reflected second-harmonic depends on satisfaction of the phase-matching condition. Comparison with those reported by Bhanthumnavin and Ampole (1990) and Bhanthumnavin and Lee (1994) shows the same feature of  $I_R(2\mathbf{w})$  dependence of  $\mathbf{q}_i$ .

### 4.3.2 Nonlinear Brewster angle of ADP with $P^{NLS}(2\mathbf{w})$ making an angle $30^\circ$ from the incident surface

According to the condition of nonlinear Brewster angle, the possibility of observation of the phenomenon of nonlinear Brewster angle in any nonlinear optical crystal is not unique as in linear case. The nonlinear Brewster angle depends on the orientation of the ( $P^{NLS}(2\mathbf{w})$ ). In order to test this statement, another crystallographic orientation, in this case the one of its optic axis making  $30^\circ$  from incident surface is considered. The condition of nonlinear Brewster for this case is

$$\mathbf{a} + \mathbf{q}_s + \mathbf{q}_r = 2\mathbf{p}$$

and

$$\mathbf{a} + \mathbf{q}_s = 300^\circ.$$

Thus

$$\begin{aligned} \mathbf{q}_r &= 360^\circ - 300^\circ \\ &= 60^\circ. \end{aligned}$$

To know the incident angle, making use of Snell's law,

$$n_{iq}(\mathbf{w}) \sin \mathbf{q}_i^{NB} = n_e^{2w}(2\mathbf{q}_r) \sin \mathbf{q}_r$$

or

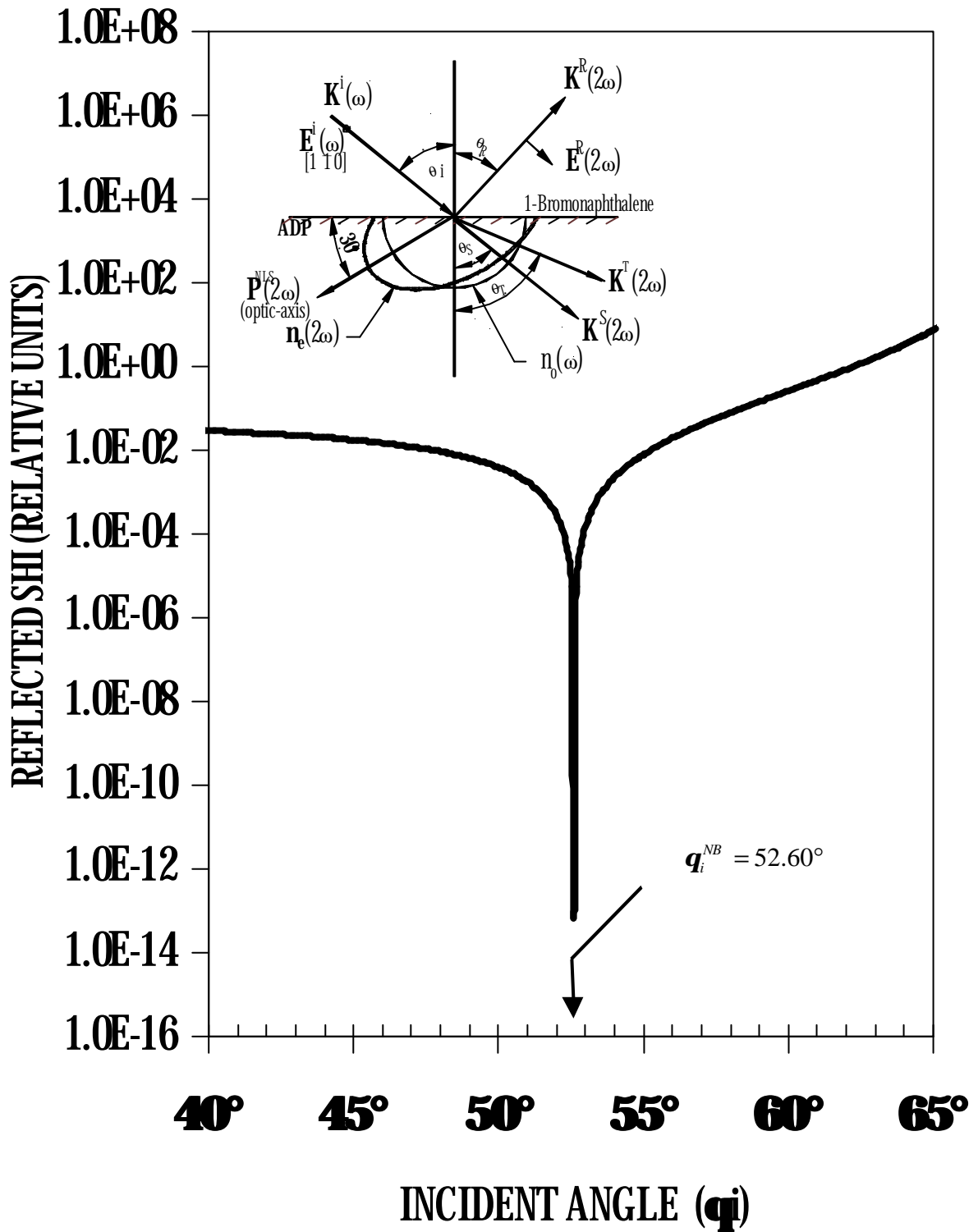


Figure 4.3. Relative reflected second-harmonic intensity (SHI) from ADP crystal as a function of  $q_i$ . Nonlinear Brewster angle is at  $q_i^{NB} = 52.60^\circ$  with  $P^{NLS}(2\omega)$  is at  $30^\circ$

$$\begin{aligned}
\mathbf{q}_i^{NB} &= \sin^{-1} \left[ \frac{n_e^{2w}(120^\circ) \sin 60^\circ}{n_{liq}(\mathbf{w})} \right] \\
&= \sin^{-1} \left[ \frac{1.4984 \sin 60^\circ}{1.6335} \right] \\
&= 52.60^\circ.
\end{aligned}$$

At  $\mathbf{q}_i = 52.60^\circ$  the reflected second-harmonic intensity is then vanish as show in Figure 4.3.

### 4.3.3 Nonlinear Brewster angle of ADP with $P^{NLS}(2\mathbf{w})$ is lies along the face normal

When the optic axis of the crystal lies along the face normal, it means that the nonlinear Brewster angle corresponds to the condition of

$$\mathbf{a} + \mathbf{q}_s + \mathbf{q}_r = 0$$

and

$$\mathbf{a} = \mathbf{q}_s = \mathbf{q}_r = 0^\circ.$$

As same as for  $\mathbf{q}_i$

$$\mathbf{q}_i^{NB} = 0^\circ.$$

This case it seems to be the trivial condition. Normally, one says that the reflected second-harmonic can be generated as long as laser light passes through the noncentrosymmetric crystal, but this statements not always true, as can see in Figure 4.4. Recall linear optics that when the normal incident from air to glass is performed, we get 4% out of reflected. However, in the nonlinear optical case of SHI in reflection, it is zero in contrast to the linear case.



### 4.3.4 Nonlinear Brewster angle of ADP with at total reflection

In section 4.2.1, one can see that at total reflection the reflected second-harmonic intensity is vary high. Under the same situation with a different orientation of the crystal, the minimum intensity of second-harmonic in reflection will occur. By cutting the crystal in such a way that its optic axis lies along the interface, the condition for nonlinear Brewster angle will be achieved if

$$\mathbf{a} + \mathbf{q}_s + \mathbf{q}_r = \mathbf{p},$$

which

$$\mathbf{a} + \mathbf{q}_s = 90^\circ.$$

One can find

$$\mathbf{q}_r = 90^\circ.$$

As long as the wave  $k^T$  reach out from the interface between 1-bromonaphthalene and ADP crystal, the reflected intensity of second-harmonic will go to zero as shows in Figure 4.5.

By Snell's law, the critical angle, which leads to zero intensity at total reflection, is

$$\begin{aligned} \mathbf{q}_i^{NB} &= \sin^{-1} \left[ \frac{n_e^{2w}(180^\circ) \sin 90^\circ}{n_{liq}(\mathbf{w})} \right] \\ &= \sin^{-1} \left[ \frac{1.5343 \sin 90^\circ}{1.6335} \right] \\ &= 69.93^\circ. \end{aligned}$$

Figure 4.5 shows that at first critical angle  $\mathbf{q}_{cr}(\mathbf{w}) = 67.76^\circ$  the intensity trends to be increase rapidly. For large angle of incident, this second-harmonic intensity eventually decreases. Until the second critical angle is approached the deepest of



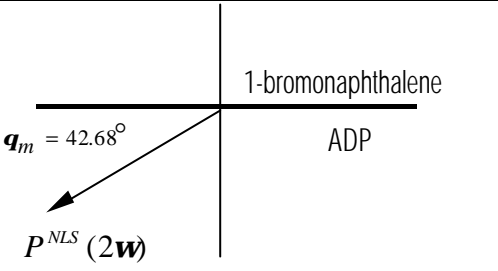
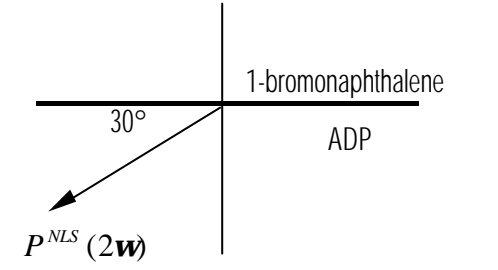
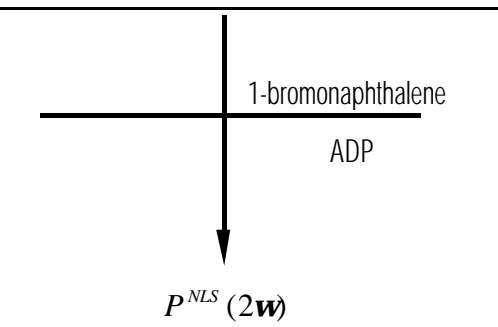
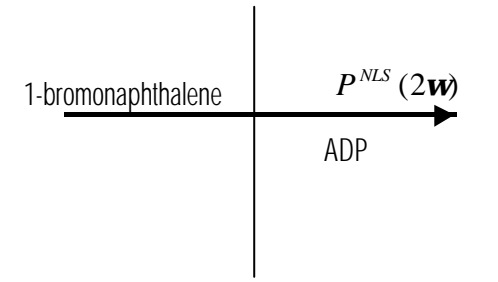
intensity is occurred. This is due to the fact that nonlinear Brewster phenomenon can be occurred when a coincidence between  $P^{NLS}(2\mathbf{w})$  and  $k^{-T}$  is accomplished.

## Chapter V

### Conclusion

The theoretical framework about behavior of optical second-harmonic generated from ADP in reflection, especially phase-mating at total reflection and the nonlinear Brewster phenomenon was studied and applied. The relative reflected second-harmonic intensity was calculated by C<sup>++</sup> program. The computer simulation was taken in two steps, the first being the calculation of refractive index of extraordinary ray  $n_e^{2w}(\mathbf{q})$  by the equation of index ellipsoid. The second step is concerned with the calculating of relative reflected second-harmonic intensity depending on the nonlinear Fresnel factor  $F_{R,II}^{NL}$  and linear Fresnel factor  $F_T^L$ . The results show that under the proposed ADP crystal orientation, the maximum and minimum of reflected second-harmonic intensity were accomplished and agree well with previous work of Bloembergen and Lee (1962); Lee and Bhanthumnavin (1976) and Bhanthumnavin and Lee (1994) of the same crystal point group. Furthermore, the results from the theoretical calculation also indicate that nonlinear Brewster angle is not unique and can have many values in a crystal depend on the orientation of  $P^{NLS}(2\mathbf{w})$  (see table 5.1).

Table 5.1. The summarized results of reflected SHI of ADP with different aspect of crystallographic cuts.

| Crystallographic orientation  | $q_i$  | $q_r$                       | $I_R(2\mathbf{w})$ |
|---|--|-----------------------------|--------------------|
|    | $q_{cr}(\mathbf{w}) = q_{cr}(2\mathbf{w}) = 67.76^\circ$<br>$q_i^{NB} = 42.02^\circ$ | $90^\circ$<br>$47.32^\circ$ | Maximum<br>Minimum |
|   | $q_i^{NB} = 52.60^\circ$   | $60^\circ$                  | Minimum            |
|  | $q_i^{NB} = 0^\circ$   | $0^\circ$                   | Minimum            |
|  | $q_i^{NB} = q_{cr}(2\mathbf{w}) = 90^\circ$  | $90^\circ$                  | Minimum            |

It is important to note that both of maximum and minimum of second-harmonic intensity occur at the same orientation of  $P^{NLS}(2\mathbf{w})$  as in the case of phase-matched at

total reflection. This is due to the fact that second-harmonic intensity is depended on the orientation of crystal.

The results provide theoretical data, which will be served as a background information for future experimental verification. The suggestion for experimental verification are as following;

1. In order to observed second harmonic signal clearly, ultrashort pulse of high peak power should be used to excite the nonlinear crystal.
2. The optically denser liquid 1-bromonaphthalene should be used for achieving total reflection condition and to prevent the deterioration of the crystal surface
3. The instrument for detecting second-harmonic signal need to be very sensitive, since it will be involved in detection of very low intensity (in the case of minimum).
4. The filter, polarizer and analyzer should be used in order to prevent our second-harmonic signal unwanted signal.

## **References**

## References

- Armstrong, J. A., Bloembergen, N., Ducuing, J. and Pershan, P. S. (1962). Interactions between light waves in a nonlinear dielectric. **Phy. Rev.** 127:1918-1939.
- Ashkin, A., Boyd, G.D. and Dziedzic J.M. (1963). Observation of continuous optical harmonic generation with gas masers. **Phys. Rev. Lett.** 11: 14.
- Bhanthumnavin, V. and Ampole, N. (1990). Theoretical prediction of nonlinear Brewster angle in ADP. **Micro. Opt. Tech. Lett.** 3: 239.
- Bhanthumnavin, V. and Lee, C.H.(1990). Reflection and transmission in second-harmonic generation of light in KDP crystal. **Micr. Opt. Tech. Lett.** 3: 279.
- Bhanthumnavin, V. and Lee, C.H. (1994). Optical second-harmonic generation of oblique incident light in transmission in potassium dihydrogen phosphate crystal. **J. Appl. Phys.** 75: 3294.
- Bhanthumnavin, V. and Lee, C. H. (1994). Optical second-harmonic generation at total reflection in a potassium dihydrogen phosphate crystal. **Phys. Rev. A.** 50:2579
- Bloembergen, N. and Pershan, P.S. (1962). Light wave at the boundary of nonlinear media. **Phys. Rev.** 128: 193.
- Bloembergen, N. (1965). **Nonlinear optics**. W. A. Benjamin, Inc. New York.
- Bloembergen, N. and Lee, C. H. (1967). Total reflection in second – harmonic generation. **Phy. Rev. Lett.** 19: 835.

- Bloembergen, N., Simon, H. J., and Lee, C. H. (1969). Total reflection phenomena in second – harmonic generation of light. **Phy. Rev.** 181: 1261.
- Boyd, G. D., Ashkin, A., Dziedzic, J. M. and Kleinman, D.A. (1965). Second – harmonic generation of light with double reflection. **Phy. Rev.** 137: 1305.
- Boyd, R. W. (1992). **Nonlinear optics**. Academic Press, Inc. Boston.
- Butcher, P. N. and Cotter, D. (1990). **The elements of nonlinear optics**. Cambridge University Press. Newcastle.
- Chang, R. K. and Bloembergen, N. (1966). Experimental verification of the laws for the reflected intensity of second – harmonic light. **Phy. Rev.** 144: 775.
- Dmitriev, V. N., Gurzadyan, G. G., and Nikogosyan, D. N. (1991). **Hanbook of nonlinear optical crystals**. Springer – Verlag: New York
- Ducuing, J. and Bloembergen, N. (1963). Observation of reflected light harmonic at the boundary of piezoelectric crystals. **Phy. Rev. Lett.** 10: 476.
- Dürr, T., Hildebrandt, R., Marowsky, G. and Stolle, R. (1997). Nonlinear Brewster angle in trasmission. **Phy. Rew. A** 56:4139.
- Franken, P. A., Hill, A. E., Peters, C. W. and Weinreich, G. (1962). Generation of optical harmonic. **Phy. Rev.** 127: 1918.
- Giordmaine, J. A. (1962). Mixing of light beam in crystals. **Phy. Rev. Lett.** 8: 19.
- He, Q. S. and Liu, S.H. (1999). **Physics of nonlinear optics**. World Scientific Publishing Co. Pte. Ltd. Singapore.
- Jenkins, F. A. and White, H. E. (1976). **Fundamentals of Optics 4<sup>th</sup> ed.** McGraw-hill., Singapore.
- Lee, C.H. and Bhanthumnavin, V. (1976). Observation of nonlinear brewster angle in KDP. **Opt. Comm.** 18: 326.

- Maker, P. D., Terhune, R. W., Nisenoff, M. and Savage, C. M. (1962). Effects of dispersion and focusing on the production of optical harmonics. **Phy. Rev. Lett.** 8: 21.
- Mills, D.L. (1991). **Nonlinear optics: basics concept**. Springer-Verlag Berlin Heidelberg. New York.
- Newell, A. C. and Moloney, J. V. (1992). **Nonlinear optics**. Addison-wesley Publishing Company. USA.
- Prasad, P. N. and Williams, D. J. (1990). **Introduction to nonlinear optical effect in molecules & polymers**. Wiley-Interscience Publication. New York
- Suripon, U. and Bhanthumnavin, V.(1999).The theoretical prediction of nonlinear Brewster angle in a potassium dihydrogen phosphate (KDP) crystal. In **25<sup>th</sup> congress on science and technology of Thailand** (558-559). Bangkok: The Science Society of Thailand under the Patronage of His Majesty the King,
- Yariv, A. (1991). **Optical Electronics 4<sup>th</sup>ed**. Saunder College Publishing, Philadelphia.
- Zernike, Jr.F. (1964).Reflective indices of ammonium dihydrogen phosphate and potassium dihydrogen phosphate between 2000 Å and 1.5 μm . **J. Opt. Soc. Am.** (54): 1215.

## **Appendix**

## Appendix A

### Derivation of Refractive Indices of 1-bromonaphthalene

The derivation of refractive indices of 1-bromonaphthalen based on the Cauchy's equation, at both 900nm ( $n_{liq}(\mathbf{w})$ ) and 450nm( $n_{liq}(2\mathbf{w})$ ) is given in this section. Due to the variation of the index of refraction with the wavelength of light passing through the material leads to the fact that  $n$  is a function of wavelength as Cauchy has been given mathematically. The refractive indices of 1-bromonaphthalene at fundamental and second-harmonic wavelength can be obtained by Cuation's equation as

$$n = A + \frac{B}{I^2} + \frac{C}{I^4}. \quad (\text{A.1})$$

Where A,B, and C are the constant. In order to find the values of A, B, and C, one have to know value of n for three different of  $I$ . Then three equations of three unknowns will be set up as a matrix form

$$\begin{bmatrix} 1 & 1/I_1^2 & 1/I_1^4 \\ 1 & 1/I_2^2 & 1/I_2^4 \\ 1 & 1/I_3^2 & 1/I_3^4 \end{bmatrix} \begin{bmatrix} A \\ B \\ C \end{bmatrix} = \begin{bmatrix} n_1 \\ n_2 \\ n_3 \end{bmatrix} \quad (\text{A.2})$$

By using the Cramer's rule, the constant A, B, and C can be solved as

$$A = \frac{\begin{vmatrix} n_1 & 1/I_1^2 & 1/I_1^4 \\ n_2 & 1/I_2^2 & 1/I_2^4 \\ n_3 & 1/I_3^2 & 1/I_3^4 \end{vmatrix}}{\begin{vmatrix} 1 & 1/I_1^2 & 1/I_1^4 \\ 1 & 1/I_2^2 & 1/I_2^4 \\ 1 & 1/I_3^2 & 1/I_3^4 \end{vmatrix}}, B = \frac{\begin{vmatrix} 1 & n_1 & 1/I_1^4 \\ 1 & n_2 & 1/I_2^4 \\ 1 & n_3 & 1/I_3^4 \end{vmatrix}}{\begin{vmatrix} 1 & 1/I_1^2 & 1/I_1^4 \\ 1 & 1/I_2^2 & 1/I_2^4 \\ 1 & 1/I_3^2 & 1/I_3^4 \end{vmatrix}}, C = \frac{\begin{vmatrix} 1 & 1/I_1^2 & n_1 \\ 1 & 1/I_2^2 & n_2 \\ 1 & 1/I_3^2 & n_3 \end{vmatrix}}{\begin{vmatrix} 1 & 1/I_1^2 & 1/I_1^4 \\ 1 & 1/I_2^2 & 1/I_2^4 \\ 1 & 1/I_3^2 & 1/I_3^4 \end{vmatrix}} \quad (\text{A.3})$$

Now the value of A, B, and C have been solved, then substitute these values in equation (A.1) and find the value of indices  $n$  at 900nm

$$n_{(900)} = A + \frac{B}{900^2} + \frac{C}{900^4}, \quad (\text{A.4})$$

and for 450nm

$$n_{(450)} = A + \frac{B}{450^2} + \frac{C}{450^4}. \quad (\text{A.5})$$

In the thesis, four sets of indices  $n$  of different wavelength are used for the calculation of the indices of 1-bromonaphthalene of both fundamental and second-harmonic frequencies. An acceptable value of  $n_{liq}$  at needed wavelength is the average value. Table A.1 and A. 2 show the sets of wavelength and indices  $n$  which corresponds to those wavelengths, used for the calculation of  $n_{liq}(\mathbf{w})$  and  $n_{liq}(2\mathbf{w})$ .

Table A.1. The sets of wavelength and indices  $n$ , used for the calculation of  $n_{liq}(\mathbf{w})$ 

| Set I                          |         | Set II                           |        | Set III                          |        | Set IV                           |        |
|--------------------------------|---------|----------------------------------|--------|----------------------------------|--------|----------------------------------|--------|
| $I$ (nm)                       | $n$     | $I$ (nm)                         | $n$    | $I$ (nm)                         |        | $I$ (nm)                         | $n$    |
| 1064*                          | 1.6262  | 1064                             | 1.6262 | 1064                             | 1.6262 | 977                              | 1.6340 |
| 532*                           | 1.6701  | 532                              | 1.6701 | 977**                            | 1.6340 | 532                              | 1.6701 |
| 486.1                          | 1.68173 | 434                              | 1.7041 | 532                              | 1.6701 | 434                              | 1.7041 |
| $n_{liq}(\mathbf{w}) = 1.6320$ |         | $n_{liq}(\mathbf{w}) = 1.631548$ |        | $n_{liq}(\mathbf{w}) = 1.642057$ |        | $n_{liq}(\mathbf{w}) = 1.636248$ |        |
| $n_{liq}(\mathbf{w}) = 1.6335$ |         |                                  |        |                                  |        |                                  |        |

\* from Bhanthumnavin and Lee (1994)

\*\* from Bloembergen, Simon, and Lee (1969)

Table A.2. The sets of wavelength and indices  $n$ , used for the calculation of  $n_{liq}(2\mathbf{w})$ .

| Set I                           |         | Set II                          |        | Set III                          |        | Set IV                           |        |
|---------------------------------|---------|---------------------------------|--------|----------------------------------|--------|----------------------------------|--------|
| $I$ (nm)                        | $n$     | $I$ (nm)                        | $n$    | $I$ (nm)                         | $n$    | $I$ (nm)                         | $n$    |
| 1064                            | 1.6262  | 1064                            | 1.6262 | 1064                             | 1.6262 | 977                              | 1.6340 |
| 532                             | 1.6701  | 532                             | 1.6701 | 977                              | 1.6340 | 532                              | 1.6701 |
| 486.1                           | 1.68173 | 434                             | 1.7041 | 532                              | 1.6701 | 488.5*                           | 1.7041 |
| $n_{liq}(\mathbf{w}) = 1.6935$  |         | $n_{liq}(\mathbf{w}) = 1.69669$ |        | $n_{liq}(\mathbf{w}) = 1.696435$ |        | $n_{liq}(\mathbf{w}) = 1.694088$ |        |
| $n_{liq}(2\mathbf{w}) = 1.6952$ |         |                                 |        |                                  |        |                                  |        |

\* from Bloembergen, Simon, and Lee (1969)

## Appendix B

### C++ Program for Calculate Relative Reflected SHI

#### B.1 $P^{NLS}$ ( $2\omega$ ) making at $\theta_m = 42.68^\circ$ with the incident surface

// C++ program for calculation of relative reflected SHI generated from ADP crystal under the excitation of ultrashort pulse laser of  $\lambda = 900\text{nm}$  (optic axis inclining at  $42.68^\circ$  from the incident surface) //

```
#include <iostream.h>
```

```
#include <math.h>
```

```
#include <iomanip.h>
```

```
#include <stdio.h>
```

```
#include <conio.h>
```

```
#include <complex.h>
```

```
complex nee(complex);
```

```
double ref(complex,complex);
```

```
int show(double, complex, double, int);
```

```
complex Oig;
```

```
void main()
```

```
{
```

```
    float AngS, AngE, AngEE, Add;
```

```
    complex OiD,OR,Os,OTT,SHI, Degg;
```

```
    complex nE2, OT, OTD;
```

```
    double x=0;
```

```
    const float nO1w=1.5120;
```

```
    const float nO2w=1.53426;
```

```
    const float nE2w=1.4870;
```

```
    const float nL1w=1.6335;
```

```
    const float nL2w=1.6952;
```

```

const float Pi=3.1415927;
complex O_s, Oi;
clrscr();
FILE *stream;
// FILE *index;
stream=fopen("SHIM.txt","w+");
// index=fopen("nADP.txt", "w+");
cout << "\n\nTransmitted Angle: Starting "; cin >> AngS;
cout << "Transmitted Angle: Ending "; cin >> AngE;
cout << "Transmitted Angle : Increasing ";cin >> Add;
cout << endl << setw(10)<< " Inci(deg) ";
cout << setw(10) << " Tran(deg)";
cout << setw(12) << " index of RDP";
cout << setw(15) << " reflected of SHI" << endl;
OTD = AngS;
AngEE = AngE;
int i=0;
while(imag(OTD) >= 90-AngEE) {
    OT=OTD*Pi/180;
    nE2=nec(OT);
    SHI = ref(OT, nE2);
    Degg = real(abs(Oig)*180/Pi);
    fprintf(stream, "%6.3lf\t%15.8lg\n", real(Degg), real(SHI));
//    fprintf(index, "%7.6lf, %7.3lf\n", nE2, Degg);
//    i = show(real(Degg), nE2, real(SHI), i);
    if(real(OTD)<90)
    {
        if(real(OTD) == 89) OTD+=0.001;
        else OTD+=Add;
    }
    else {
        if(imag(OTD) > -1) x-=0.001;

```

```

        else x-=Add;
        OTD=complex(90, x);
    }
}
fclose(stream);
// fclose(index);
cout << "Completely Calculating";
getch();
}

complex nee(complex OT)
{
    complex O_s,ss, xx;
    const float nL1w= 1.6335;
    const float nO2w = 1.53426;
    const float nE2w = 1.4870;
    const float nO1w = 1.5120;
    const float pii =3.1415927;
    xx=1/sqrt(pow(cos(47.32*pii/180+OT),2)/(nO2w*nO2w)+pow(sin
(47.32*pii/180+OT),2)/(nE2w*nE2w));
    complex nE2 = abs(xx);
    return nE2;
}

double ref(complex O_t, complex nE2)
{
    complex tt;
    const float Piii=3.1415927;
    const float nO1w=1.5120;
    const float nL1w=1.6335;
    const float nL2w=1.6952;

```

```

complex ii=nE2*sin(O_t)/nL1w;
complex Oi=asin(ii);
Oig = real(abs(Oi));
Oi = Oig;
complex OR=asin(nL1w*sin(Oi)/nL2w);
complex ss = nL1w*sin(Oi)/nO1w;
complex O_s = asin(ss);
complex crit_w=asin(nO1w/nL1w);
complex FLm =2*cos(Oi)/((sin(crit_w)*cos(O_s))+cos(Oi));
complex FNLm=(sin(O_s)*sin(O_t)*sin(O_t)*sin(O_t+(312.68*Piii/180)))/
(sin(OR)*sin(O_t+OR)*cos(O_t-OR)*sin(O_t+O_s));
double Ir=real(abs(pow(abs(FLm), 4.0)*pow(abs(FNLm), 2.0)*cos(OR)/
cos(Oi)));
return Ir;
}

int show(double Degg, complex nE2, double SHI, int i)
{
    printf("%8.3lf |", Degg);
    printf("%10.6lf |", real(nE2));
    printf("%15.8lg \n",SHI);
    if(i>20)
    { i=0;
    getch();
    }
    i++;
    return i;
}

```

## B.2 $P^{NLS}$ (2w) making at 30° with the incident surface

```
// C++ program for calculation of relative reflected SHI generated from ADP crystal under the
excitation of ultrashort pulse laser of  $\lambda = 900\text{nm}$  (optic axis inclining at 30° from the incident
surface) //
#include <iostream.h>
#include <math.h>
#include <iomanip.h>
#include <stdio.h>
#include <conio.h>
#include <complex.h>
complex nee(complex);
double ref(complex,complex);
int show(double, complex, double, int);
complex Oig;
void main()
{
    float AngS, AngE, AngEE, Add;
    complex OiD,OR,Os,OTT,SHI, Degg;
    complex nE2, OT, OTD;
    double x=0;
    const float nO1w=1.5120;
    const float nO2w=1.53426;
    const float nE2w=1.4870;
    const float nL1w=1.6335;
    const float nL2w=1.6952;
    const float Pi=3.1415927;
    complex O_s, Oi;
    clrscr();
    FILE *stream;
//    FILE *index;
    stream=fopen("SHIM.txt","w+");
//    index=fopen("nADP.txt", "w+");
```

```

cout << "\n\nTransmitted Angle: Starting "; cin >> AngS;
cout << "Transmitted Angle: Ending "; cin >> AngE;
cout << "Transmitted Angle : Increasing ";cin >> Add;
cout << endl << setw(10)<< " Inci(deg) ";
cout << setw(10) << " Tran(deg)";
cout << setw(12) << " index of RDP";
cout << setw(15) << " reflected of SHI" << endl;
OTD = AngS;
AngEE = AngE;
int i=0;
while(imag(OTD) >= 90-AngEE) {
    OT=OTD*Pi/180;
    nE2=nec(OT);
    SHI = ref(OT, nE2);
    Degg = real(abs(Oig)*180/Pi);
    fprintf(stream, "%6.3lf\t%15.8lg\n", real(Degg), real(SHI));
    fprintf(index, "%7.6lf, %7.3lf\n", nE2, Degg);
    i = show(real(Degg), nE2, real(SHI), i);
    if(real(OTD)<90)
    {
        if(real(OTD) == 89) OTD+=0.001;
        else OTD+=Add;
    }
    else {
        if(imag(OTD) > -1) x-=0.001;
        else x-=Add;
        OTD=complex(90, x);
    }
}
fclose(stream);
// fclose(index);
cout << "Completely Calculating";

```

```

    getch();
}

complex nee(complex OT)
{
    complex O_s,ss, xx;
    const float nL1w= 1.6335;
    const float nO2w = 1.53426;
    const float nE2w = 1.4870;
    const float nO1w = 1.5120;
    const float pii =3.1415927;
    xx=1/sqrt(pow(cos(60*pii/180+OT),2)/(nO2w*nO2w)+pow(sin
(60*pii/180+OT),2)/(nE2w*nE2w));
    complex nE2 = abs(xx);
    return nE2;
}

double ref(complex O_t, complex nE2)
{
    complex tt;
    const float Piii=3.1415927;
    const float nO1w=1.5120;
    const float nL1w=1.6335;
    const float nL2w=1.6952;
    complex ii=nE2*sin(O_t)/nL1w;
    complex Oi=asin(ii);
    Oig = real(abs(Oi));
    Oi = Oig;
    complex OR=asin(nL1w*sin(Oi)/nL2w);
    complex ss = nL1w*sin(Oi)/nO1w;
    complex O_s = asin(ss);
}

```

```

complex crit_w=asin(nO1w/nL1w);
complex FLm =2*cos(Oi)/((sin(crit_w)*cos(O_s))+cos(Oi));
complex FNLM=(sin(O_s)*sin(O_t)*sin(O_t)*sin(O_t+(300*Piii/180)))/
(sin(OR)*sin(O_t+OR)*cos(O_t-OR)*sin(O_t+O_s));
double Ir=real(abs(pow(abs(FLm), 4.0)*pow(abs(FNLM), 2.0)*cos(OR)/
cos(Oi)));
return Ir;
}

int show(double Degg, complex nE2, double SHI, int i)
{
    printf("%8.3lf |", Degg);
    printf("%10.6lf |", real(nE2));
    printf("%15.8lg \n",SHI);
    if(i>20)
    { i=0;
    getch();
    }
    i++;
    return i;
}

```

### B.3 $P^{NLS}$ (2w) making at $0^\circ$ with the face normal

// C++ program for calculation of relative reflected SHI generated from ADP crystal under the excitation of ultrashort pulse laser of  $\lambda = 900\text{nm}$  (optic axis inclining at  $0^\circ$  from the face normal) //

```
#include <iostream.h>
#include <math.h>
#include <iomanip.h>
#include <stdio.h>
#include <conio.h>
#include <complex.h>

complex nee(complex);
double ref(complex,complex);
int show(double, complex, double, int);
complex Oig;
void main()
{
    float AngS, AngE, AngEE, Add;
    complex OiD,OR,Os,OTT,SHI, Degg;
    complex nE2, OT, OTD;
    double x=0;
    const float nO1w=1.5120;
    const float nO2w=1.53426;
    const float nE2w=1.4870;
    const float nL1w=1.6335;
    const float nL2w=1.6952;
    const float Pi=3.1415927;
    complex O_s, Oi;
    clrscr();
    FILE *stream;
    FILE *index;
    stream=fopen("SHI0.txt","w+");
```

```

index=fopen("nADP.txt", "w+");
cout << "\n\nTransmitted Angle: Starting "; cin >> AngS;
cout << "Transmitted Angle: Ending "; cin >> AngE;
cout << "Transmitted Angle : Increasing ";cin >> Add;
cout << endl << setw(10)<< " Inci(deg) ";
cout << setw(12) << " index of ADP";
cout << setw(15) << " Reflected SHI" << endl;
OTD = AngS;
AngEE = AngE;
int i=0;
while(imag(OTD) >= 90-AngEE) {
    OT=OTD*Pi/180;
    nE2=nec(OT);
    SHI = ref(OT, nE2);
    Degg = real(abs(Oig)*180/Pi);
    if(real(OTD) < 0) Degg = -Degg;
    fprintf(stream, "%6.3lf\t%15.8lg\n", real(Degg), real(SHI));
    fprintf(index, "%7.6lf, %7.3lf\n", nE2, Degg);
    i = show(real(Degg), nE2, real(SHI), i);
    if(real(OTD)<90)
    {
        if(real(OTD) == 89) OTD+=0.01;
        else OTD+=Add;
    }
    else {
        if(imag(OTD) > -1) x-=0.01;
        else x-=Add;
        OTD=complex(90, x);
    }
}
fclose(stream);
fclose(index);

```

```

    cout << "Completely Calculating";
    getch();
}

complex nee(complex OT)
{
    complex O_s,ss, xx;
    const float nL1w= 1.6335;
    const float nO2w = 1.6952;
    const float nE2w = 1.4870;
    const float nO1w = 1.5120;
    const float pii =3.1415927;
    xx=1/sqrt(pow(cos(OT),2)/(nO2w*nO2w)+pow(sin(OT),2)/(nE2w*nE2w));
    complex nE2 = abs(xx);
    return nE2;
}

double ref(complex O_t, complex nE2)
{
    complex tt;
    const float Piii=3.1415927;
    const float nO1w=1.5120;
    const float nL1w=1.6335;
    const float nL2w=1.6952;
    complex ii=nE2*sin(O_t)/nL1w;
    complex Oi=asin(ii);
    Oig = real(Oi);
    Oi = Oig;
    complex OR=asin(nL1w*sin(Oi)/nL2w);
    complex ss = nL1w*sin(Oi)/nO1w;
    complex O_s = asin(ss);
    complex crit_w=asin(nO1w/nL1w);
}

```

```

complex FLm =2*cos(Oi)/((sin(crit_w)*cos(O_s))+cos(Oi));
complex FNLM=(sin(O_s)*sin(O_t)*sin(O_t)*sin(O_t)/
              (sin(OR)*sin(O_t+OR)*cos(O_t-OR)*sin(O_t+O_s));
double Ir=real(abs(pow(abs(FLm), 4.0)*pow(abs(FNLM), 2.0)*cos(OR)/
              cos(Oi)));
return Ir;
}

int show(double Degg, complex nE2, double SHI, int i)
{
    printf("%8.3lf |", Degg);
    printf("%10.6lf |", real(nE2));
    printf("%15.8lg \n",SHI);
    if(i>20)
    { i=0;
      getch();
    }
    i++;
    return i;
}

```

#### B.4 $P^{NLS}$ (2w) making at 90° with the face normal

// C++ program for calculation of relative reflected SHI generated from ADP crystal under the excitation of ultrashort pulse laser of  $\lambda = 900\text{nm}$  (optic axis inclining at 90° from the face normal) //

```
#include <iostream.h>
#include <math.h>
#include <iomanip.h>
#include <stdio.h>
#include <conio.h>
#include <complex.h>

complex nee(complex);
double ref(complex,complex);
int show(double, complex, double, int);
complex Oig;
void main()
{
    float AngS, AngE, AngEE, Add;
    complex OiD,OR,Os,OTT,SHI, Degg;
    complex nE2, OT, OTD;
    double x=0;
    const float nO1w=1.5120;
    const float nO2w=1.53426;
    const float nE2w=1.4870;
    const float nL1w=1.6335;
    const float nL2w=1.6952;
    const float Pi=3.1415927;
    complex O_s, Oi;
    clrscr();
    FILE *stream;
    FILE *index;
    stream=fopen("SHI90.txt","w+");
```

```

index=fopen("nADP.txt", "w+");
cout << "\n\nTransmitted Angle: Starting "; cin >> AngS;
cout << "Transmitted Angle: Ending "; cin >> AngE;
cout << "Transmitted Angle : Increasing ";cin >> Add;
cout << endl << setw(10)<< " Inci(deg) ";
cout << setw(12) << " index of ADP";
cout << setw(15) << " reflected SHI" << endl;
OTD = AngS;
AngEE = AngE;
int i=0;
while(imag(OTD) >= 90-AngEE) {
    OT=OTD*Pi/180;
    nE2=nee(OT);
    SHI = ref(OT, nE2);
    Degg = real(abs(Oig)*180/Pi);
    fprintf(stream, "%6.3lf\t%15.8lg\n", real(Degg), real(SHI));
    fprintf(index, "%7.6lf, %7.3lf\n", nE2, Degg);
    i = show(real(Degg), nE2, real(SHI), i);
    if(real(OTD)<90)
    {
        if(real(OTD) == 89) OTD+=0.001;
        else OTD+=Add;
    }
    else {
        if(imag(OTD) > -1) x-=0.001;
        else x-=Add;
        OTD=complex(90, x);
    }
}
fclose(stream);
fclose(index);
cout << "Completely Calculating";

```

```

    getch();
}

complex nee(complex OT)
{
    complex O_s,ss, xx;
    const float nL1w= 1.6335;
    const float nO2w = 1.53426;
    const float nE2w = 1.4870;
    const float nO1w = 1.5120;
    const float pii =3.1415927;
    xx=1/sqrt(pow(cos(90.00*pii/180-OT),2)/(nO2w*nO2w)+pow(sin
(90.00*pii/180-OT),2)/(nE2w*nE2w));
    complex nE2 = abs(xx);
    return nE2;
}

double ref(complex O_t, complex nE2)
{
    complex tt;
    const float Piii=3.1415927;
    const float nO1w=1.5087;
    const float nL1w=1.6298;
    const float nL2w=1.6781;
    complex ii=nE2*sin(O_t)/nL1w;
    complex Oi=asin(ii);
    Oig = real(abs(Oi));
    Oi = Oig;
    complex OR=asin(nL1w*sin(Oi)/nL2w);
    complex ss = nL1w*sin(Oi)/nO1w;
    complex O_s = asin(ss);
    complex crit_w=asin(nO1w/nL1w);

```

```

    complex FLm =2*cos(Oi)/((sin(crit_w)*cos(O_s))+cos(Oi));
    complex FNLM=(sin(O_s)*sin(O_t)*sin(O_t)*sin(O_t+(90.00*Piii/180)))/
        (sin(OR)*sin(O_t+OR)*cos(O_t-OR)*sin(O_t+O_s));
    double Ir=real(abs(pow(abs(FLm), 4.0)*pow(abs(FNLM), 2.0)*cos(OR)/
        cos(Oi)));
    return Ir;
}

int show(double Degg, complex nE2, double SHI, int i)
{
    printf("%8.3lf |", Degg);
    printf("%10.6lf |", real(nE2));
    printf("%15.8lg \n",SHI);
    if(i>20)
    { i=0;
      getch();
    }
    i++;
    return i;
}

```

## **Biography**

Miss Ubon Suripon was born on 22<sup>nd</sup> May 1974 in Buriram, Thailand. She graduated from Suranaree University of Technology with a degree in Telecommunication Engineering in 1997. In 1998 she started her studies for a master's degree in Laser technology and Photonics, Institute of Science, Suranaree University of Technology where she was a teaching assistant in mathematics (calculus) for four semesters.